

THERMALLY STIMULATED CONDUCTIVITY OF ZINC-
DOPED POLYCRYSTALLINE STANNIC OXIDE

By

JOHN ALLEN FREEMAN

Bachelor of Science

Oklahoma State University

Stillwater, Oklahoma

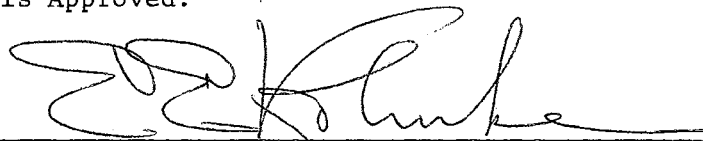
1966

Submitted to the Faculty of the Graduate College
of the Oklahoma State University
in partial fulfillment of the requirements
for the Degree of
MASTER OF SCIENCE
May, 1969

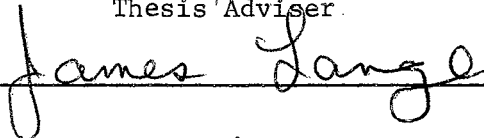
SEP 29 1969

THERMALLY STIMULATED CONDUCTIVITY OF ZINC-
DOPED POLYCRYSTALLINE STANNIC OXIDE

Thesis Approved:



Thesis Adviser



Dean of the Graduate College

724838

ACKNOWLEDGMENTS

The author is much indebted to Dr. E. E. Kohnke and would like to express appreciation for his supervision, encouragement and patience throughout the preparation of this report. Credit should also go to Dr. H. E. Matthews for the design of the basic experimental equipment and for the preparation of the samples used in this study.

TABLE OF CONTENTS

Chapter	Page
I. INTRODUCTION.	1
II. THEORETICAL BACKGROUND AND EXPERIMENTAL TECHNIQUES. . . .	4
Experimental Techniques.	8
III. APPARATUS	10
Samples.	17
IV. RESULTS	18
V. DISCUSSION AND CONCLUSIONS.	40
Discussion of Results in Fix-B Samples	40
Discussion of Results in Fix-A Samples	44
Comparison with TSL Peaks.	45
Discussion of DTSC Results	46
Additional Comments and Suggestions for Further Study.	47
BIBLIOGRAPHY.	48

LIST OF TABLES

Table	Page
I. Fix-B Activation Energies (DTSC) as a Function of Decay Temperature.	34
II. Break Temperatures for Peak (2) as a Function of Decay Temperature	37
III. Relevant Data for the Figures in Chapter IV.	41

LIST OF FIGURES

Figure	Page
1. Simple Band Model of an n-type Semiconductor	5
2. Gas Handling System	11
3. Cryostat Sample Holder System	12
4. Electrical Measurements-Heater System	14
5. Sample Holder	16
6. Thermally Stimulated Current of a Fix-B Sample Heated for 47 Hrs at 10 Microns ($3131\overset{\circ}{\text{Å}}$)	19
7. Thermally Stimulated Current of a Fix-B Sample Heated for 46.5 Hrs at 12 Microns ($3131\overset{\circ}{\text{Å}}$)	20
8. Thermally Stimulated Current of a Fix-B Sample Heated for 10 Hrs in Air ($3131\overset{\circ}{\text{Å}}$)	21
9. Thermally Stimulated Current of a Fix-B Sample Heated for 46.5 Hrs at 12 Microns ($2536\overset{\circ}{\text{Å}}$)	23
10. Thermally Stimulated Current of a Fix-B Sample Heated for 10 Hrs in Air ($2536\overset{\circ}{\text{Å}}$)	24
11. Thermally Stimulated Current of a Fix-A Sample Heated for 120 Hrs at 8 Microns ($3131\overset{\circ}{\text{Å}}$)	25
12. Thermally Stimulated Current of a Fix-A Sample Heated for 114 Hrs at 10 Microns ($3131\overset{\circ}{\text{Å}}$)	26
13. Thermally Stimulated Current of a Fix-A Sample Heated for 114 Hrs at 10 Microns ($2536\overset{\circ}{\text{Å}}$)	27
14. Excitation While Cooling-Thermally Stimulated Current of a Fix-B Sample Heated for 47 Hrs at 10 Microns ($3131\overset{\circ}{\text{Å}}$) . . .	28
15. Excitation While Cooling-Thermally Stimulated Current of a Fix-B Sample Heated for 92.5 Hrs at 10 Microns ($3131\overset{\circ}{\text{Å}}$) . .	29

LIST OF FIGURES (Continued)

Figure	Page
16. Excitation While Cooling-Thermally Stimulated Current of a Fix-B Sample Heated for 46.5 Hrs at 12 Microns (2536 $\overset{\circ}{\text{A}}$) . .	31
17. Excitation While Cooling-Thermally Stimulated Current of a Fix-A Sample Heated for 114 Hrs at 10 Microns (3131 $\overset{\circ}{\text{A}}$) . .	32
18. Excitation While Cooling-Thermally Stimulated Current of a Fix-A Sample Heated for 114 Hrs at 10 Microns (2536 $\overset{\circ}{\text{A}}$) . .	33
19. Decayed Thermally Stimulated Current Versus $10^3/T$ for Peak (1) of a Fix-B Sample Heated for 44 Hrs in Air (3131 $\overset{\circ}{\text{A}}$) . .	35
20. Decayed Thermally Stimulated Current Versus $10^3/T$ for Peak (2) of a Fix-B Sample Heated for 48.5 Hrs at 10 Microns (3131 $\overset{\circ}{\text{A}}$)	36
21. Decayed Thermally Stimulated Current Versus $10^3/T$ for Peak (1) of a Fix-A Sample Heated for 114 Hrs at 10 Microns (2536 $\overset{\circ}{\text{A}}$)	38
22. Decayed Thermally Stimulated Current Versus $10^3/T$ for Peak (2) of a Fix-A Sample Heated for 114 Hrs at 10 Microns (2536 $\overset{\circ}{\text{A}}$)	39

CHAPTER I

INTRODUCTION

Stannic oxide has been the object of research since the early 1900's, but as yet a thorough understanding of its electrical and optical properties does not exist. Studies have been made of several forms of stannic oxide, including single crystals, ceramics, thin films, pressed powders, and natural crystals. A recent extensive bibliography of the research done on this metal oxide is given by Peterson¹. Pure stannic oxide in thermodynamic equilibrium at room temperature is an electrical insulator. However, a study of its electrical properties shows that it can exhibit some properties of a semiconductor. It is, in fact, these semiconducting properties and their implications which have engaged the attention of a group at Oklahoma State University. The work reported here is part of a continuing study being carried out by that group.

Since World War II a series of experimental methods under the general heading of "photoelectronic analyses" has been applied to semiconductors to identify significant parameters. Two pertinent studies which are carried out on photoconducting semiconductors involve the thermal release of electrons trapped in defect states in the forbidden energy gap. These are the thermally stimulated currents method (TSC) and the thermally stimulated luminescence method (TSL), both of which have been used in this laboratory. The TSC method in particular has been effec-

tively used to determine electron trapping parameters. A recent paper on cadmium sulfo-selenide by Bube² indicates that in addition to trap energies, such things as capture cross sections, trap densities and the Fermi level can be determined if certain models are accepted. Trap depths have also been investigated in cadmium sulfide by Kulp³ using a range of wavelengths in the TSC measurements. The general validity of the initial rise method of TSC analysis applied in the present study has been questioned by some authors and several recent papers^{4,5,6,7} have appeared comparing various methods of analyzing TSC curves.

Locally, Houston^{8,9} and Matthews¹⁰ have used the TSC method to investigate the defect states in single-crystal and zinc-doped polycrystalline stannic oxide respectively, between -160°C and $+100^{\circ}\text{C}$ and each provides an extensive bibliography of studies employing this method. Eagleton¹¹ has recently completed work on thermally stimulated luminescence of several forms of stannic oxide and has attempted to correlate his results with TSC data. A bibliography of past TSL studies is given in his report.

The work reported here was an extended investigation of the defect states of 0.7% zinc-doped stannic oxide from -180°C to 0°C . The methods of thermally stimulated currents and two modifications of this method, to be described later, were used. It was hoped that quantitative values of the activation energies and the physical location, whether near the surface or in the bulk, of defects in stannic oxide could be determined. A further concern was the temperature at the TSC peaks. An attempt was also made to correlate these findings with the TSL results of Eagleton.

Chapter II presents the necessary theoretical background and the experimental apparatus is described in Chapter III. The experimental

results are given in Chapter IV and the conclusions are presented in Chapter V.

CHAPTER II

THEORETICAL BACKGROUND AND EXPERIMENTAL TECHNIQUES

A simple picture of the possible energy states of a solid comes from a quantum mechanical analysis of the behavior of an electron in the field of a periodic lattice. From this comes the idea that the energy states in pure semiconductors and insulators fall into a series of quasi-continuous bands. Of main importance to the electrical conduction processes are two of these, one (valence band) filled with electrons and the other (conduction band) empty at absolute zero. These are separated by a "forbidden" energy gap which for a perfect crystal has no electronic states.

A convenient way to visualize these two main bands is the flat-band picture shown in Figure 1. For purposes of illustration, it is assumed there exist in the forbidden gap N_d donor states per unit volume with an activation energy E_d and an occupation density of electrons n_d , plus N_a acceptor states per unit volume with an occupation density of electrons n_a . It is assumed that $N_d > N_a$ and that those electrons contributing to the conduction process come from the donor levels. Such donor levels can act as traps or recombination centers depending on the occupancy of the conduction band by electrons, their capture cross section S_n and the average electron velocity \bar{v} . A complete discussion differentiating traps and recombination centers for non-equilibrium processes such as

are of prime interest in the work reported here is provided by Bube⁽¹²⁾. The following analysis will emphasize the kinetics of trapping and recombination for the purpose of deriving basic expressions of a type which can be used in the consideration of experimental data and the identification of important parameters. Electrons can be thermally ex-

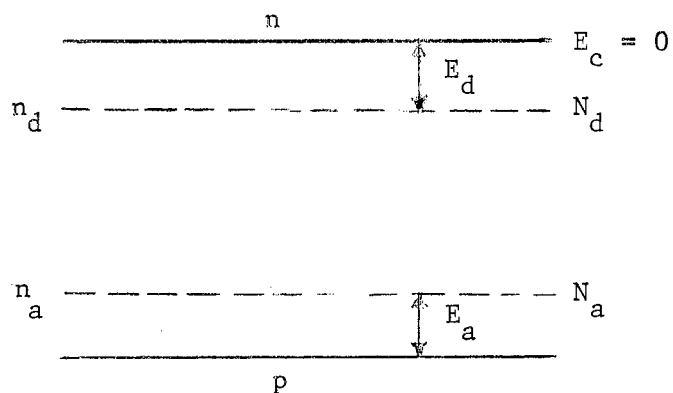


Figure 1. Simple Band Model of an n-Type Semiconductor

cited out of traps at a rate given by

$$n_d \nu \exp(-E_d/KT) \quad (1)$$

where ν is the attempt-to-escape frequency. As can be shown⁽¹²⁾, there exists a relation, independent of the model chosen, which involves ν , S_n and \bar{V} :

$$N_c S_n \bar{V} = \nu \quad (2)$$

where $N_c = 2 \left[\frac{2\pi M_e KT}{h^2} \right]^{3/2}$ and M_e is the effective mass for electrons.

In the present work, the method of thermally stimulated currents

(TSC) is used. This involves the photo-excitation of electrons from the valence band to the conduction band at a low temperature, followed by a decay time during which the light is turned off and the electrons are allowed to recombine with holes or become trapped in energy states in the band gap. This establishes a non-equilibrium density of electrons in these traps which is then relieved by raising the temperature. The density of conduction electrons, as indicated by the sample current, increases and passes through a maximum under the influence of the competing processes of detrapping and recombination during this temperature rise. The rate of thermal excitation is assumed to follow the equation:

$$\frac{dn_t}{dt} = n_t \nu \exp(-E_t/KT) \quad (3)$$

or using equation (2),

$$\frac{dn_t}{dt} = n_t N_c S_n \bar{v} \exp(-E_t/KT) \quad (3')$$

where n_t is the density of trapped electrons and E_t is their activation energy measured from the bottom of the conduction band. Taking into account the recombination process, the differential equation for the change in the density of conduction electrons (n) with time is expressed in terms of equation (3) and their average lifetime (recombination parameter) τ , giving

$$\frac{dn}{dt} = \frac{dn_t}{dt} - n/\tau \quad (4)$$

This equation neglects the retrapping which could occur during time τ .

It is generally assumed that $\frac{dn}{dt}$ is much smaller than the other rates

for rates of temperature rise normally used. Therefore, equation (4) becomes

$$\frac{dn_t}{dt} \approx n/\tau \quad (5)$$

The activation energy E_t can be determined in a number of ways⁽⁶⁾.

The most widely used approach is that of Garlick and Gibson⁽¹³⁾ using the fact that the TSC rises exponentially on the low temperature approach to its peak. If a linear heating rate (b) is used then

$T(t) = T_0 + bt$ and $\frac{dn_t}{dt} = b \frac{dn_t}{dT}$, so equation (5) becomes

$$b \frac{dn_t}{dT} \approx \frac{n(T)}{\tau} \quad (6)$$

Using equation (3') this becomes:

$$n(T) \approx b \tau n_t(T) N_c S_n \bar{V} \exp(-E_t/KT) \quad (7)$$

As long as the coefficient $b \tau n_t(T) N_c S_n \bar{V}$ varies slowly with temperature, a plot of $\log n(T)$ versus $1/T$ has a slope equal to $(-E_t/K)$.

In practice either the conductivity (σ) or the sample current (i) is known where:

$$\sigma = ne\mu = \frac{i l}{VB} \quad (8)$$

where e is the charge of an electron, μ is the free electron mobility, V is the applied voltage and l and B are the length and cross-sectional area of the sample. Therefore, a plot of $\log(i)$ versus $1/T$ will have a slope essentially equal to $(-E_t/K)$ if the mobility remains constant or varies slowly with temperature.

This analysis can be applied to individual trapping levels when

several are present if these levels are widely-spaced in energy. When two or more levels are close in energy, however, overlapping peaks can occur. Special experimental techniques (DTSC) as described below can be used to provide data in a form such that the "initial rise" analysis can still be used.

Experimental Techniques

The data in this study resulted from the application of three experimental techniques: (1) Thermally stimulated currents (TSC); (2) Excitation while cooling-thermally stimulated currents (EWC-TSC), and (3) Decayed thermally stimulated currents (DTSC).

The thermally stimulated current measurement consisted of several minutes of sample irradiation with ultraviolet light near liquid nitrogen temperature, followed, after the photoconductivity was allowed to decay, by a constant rate of temperature rise. A Sargent strip chart recorder was used to monitor the temperature which was maintained within 5% of linearity by reostatically varying the heater current. Simultaneously, on a second Sargent strip chart recorder, the sample current was monitored. Following the TSC run the sample was heated to about 100°C and allowed to come to thermal equilibrium to essentially free all trapped electrons from higher-lying donor levels. Thereupon the sample was re-cooled and a run was made without illumination to obtain the dark current versus temperature. The final analysis of the TSC data involved the subtraction of the dark current from the current obtained in the TSC run to get the true thermally stimulated current.

The excitation while cooling-thermally stimulated currents technique is nearly self-explanatory. The procedure was the same as in a

TSC run except excitation was initiated during the cooling process. The sample was thereby irradiated for about thirty minutes prior to a run and the sample currents were increased accordingly.

The decayed thermally stimulated current technique involved thermally decaying out those peaks below the desired peak by raising the temperature, after illumination, to a value about 10°C below this peak. After allowing time for all lower energy traps to empty, the sample was re-cooled and a normal TSC run made. The Garlick and Gibson method was then used to calculate the energy. This method circumvents the problem of overlapping peaks.

CHAPTER III

APPARATUS

The apparatus consisted of four main parts: The gas handling system, the cryostat-sample holder, the illumination system, and the electrical measurements and heater system. A block diagram of the gas handling system is shown in Figure 2. This system allowed evacuation of the cryostat to about 10 microns pressure and provided a means of letting dry ambient gas into the sample chamber. One drying trap and one silica gel drying tube were used to insure extraction of water from the entering gas. The two-way glass valve allowed the cryostat and sample holder to be evacuated by the fore pump or to be filled with a dry ambient. After either of these actions, the valve could be rotated a quarter of a turn to leave the cryostat and sample holder completely isolated from the fore pump and gas inlet section. During the sample fixing process (heating at 100°C), the pressure was monitored by the thermocouple gage (T.G. in Figure 2) and the Veeco Vacuum Gage meter.

The cryostat-sample holder, made following suggestions by Matthews (10), is shown in Figure 3. The two main parts were (1) the brass vacuum chamber with a quartz optical port and a gas port, and (2) a stainless steel dewar with a sample and heater chamber and a guard tube. These two parts were joined using an "O" ring and C-clamps. All joints of the vacuum chamber were soldered and the quartz window was sealed in the optical port with Apiezon W vacuum wax. A thermocouple gage was

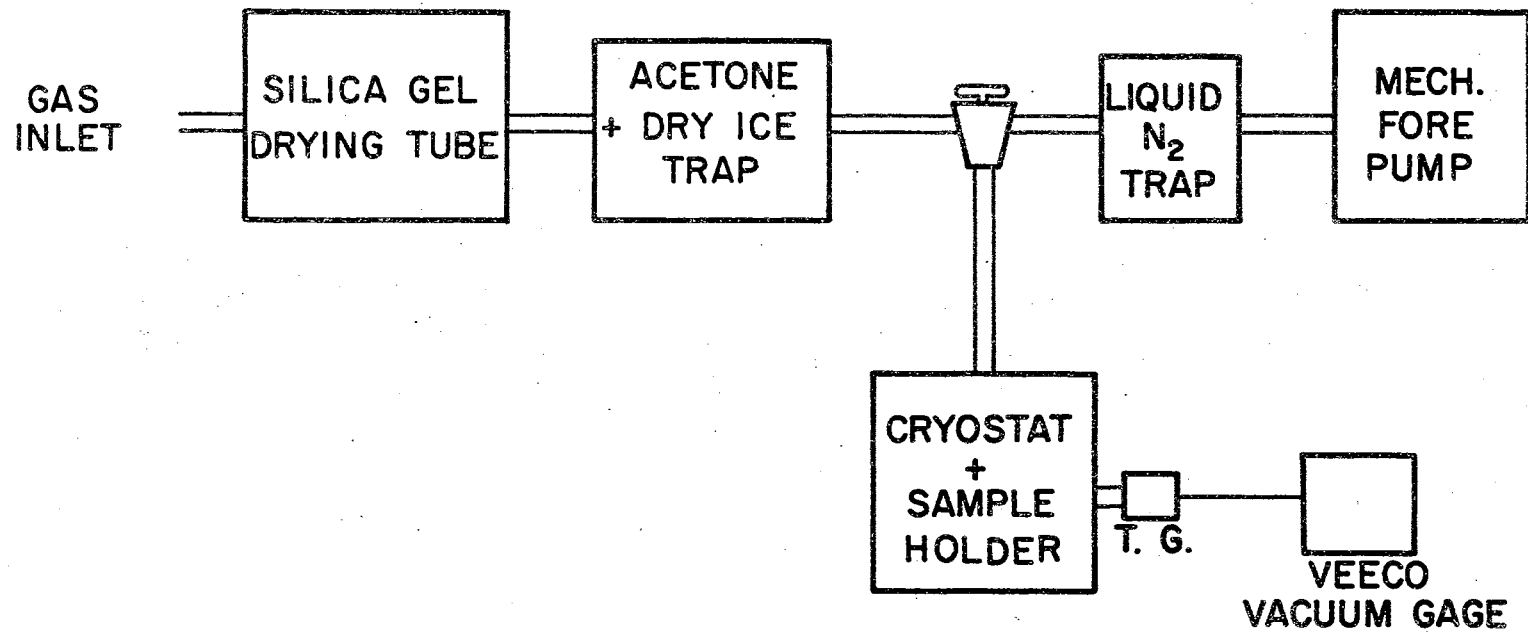


Figure 2. Gas Handling System

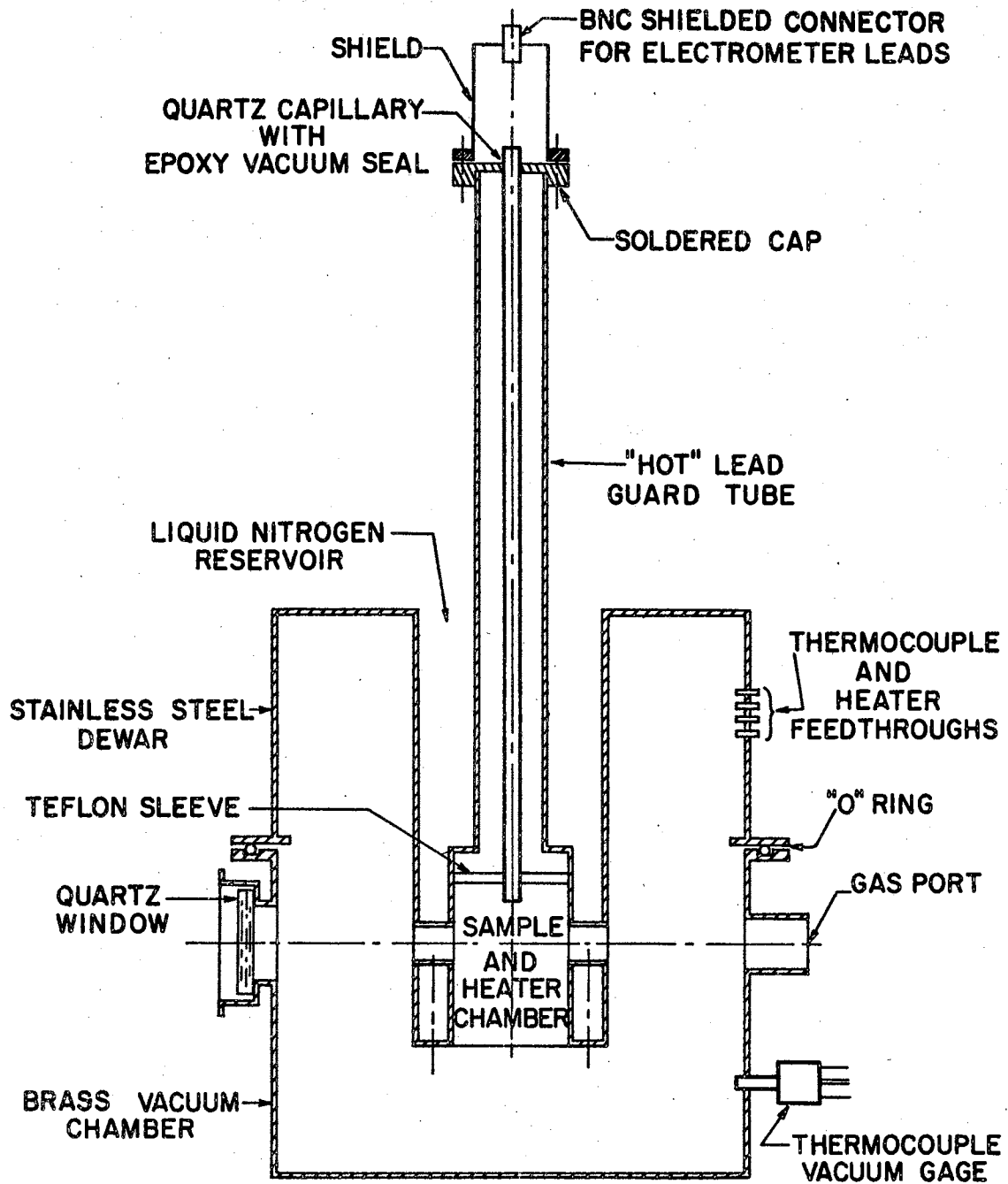


Figure 3. Cryostat Sample Holder System .

mounted in the side of this chamber to monitor the pressure.

The stainless steel dewar was designed to cool the sample chamber as well as to allow for the illumination of the sample with light. Liquid nitrogen was introduced into the reservoir and with the aid of a copper base plate (shown in Figure 5) mounted on the bottom of the dewar, heat could be conducted away from the sample. A second thermal path was provided by introducing a gas such as helium, nitrogen, or air into the cryostat. Two ports from the sample and heater chamber to the outer walls of the liquid nitrogen reservoir allowed for the evacuation of this chamber and provided a path for light from an external source to fall on the sample. The stainless steel guard tube extended 24 inches above the sample and heater chamber to allow the "hot" lead to be brought out of the dewar at a position which was thermally and electrically isolated. An additional brass shield was mounted with screws to a brass cap atop the stainless steel guard tube. A quartz capillary rod was vacuum-sealed with epoxy into a hole in the brass cap and further supported at the bottom of the guard tube by a teflon sleeve. This quartz capillary provided an insulated path for the "hot" lead which was brought out at the BNC shielded connector. All joints of the stainless steel dewar were welded to reduce the chance of the joints cracking during the thermal cycling of the system. Four feedthroughs were placed in the side of the dewar to allow the heater and thermocouple leads to be brought to the outside. These feedthroughs were positioned as far from the liquid nitrogen chamber as possible to reduce the temperature gradient in their vicinity.

The circuit for the electrical measurements and heater system is shown in Figure 4. Two thermocouple connectors, Type #040433, made by

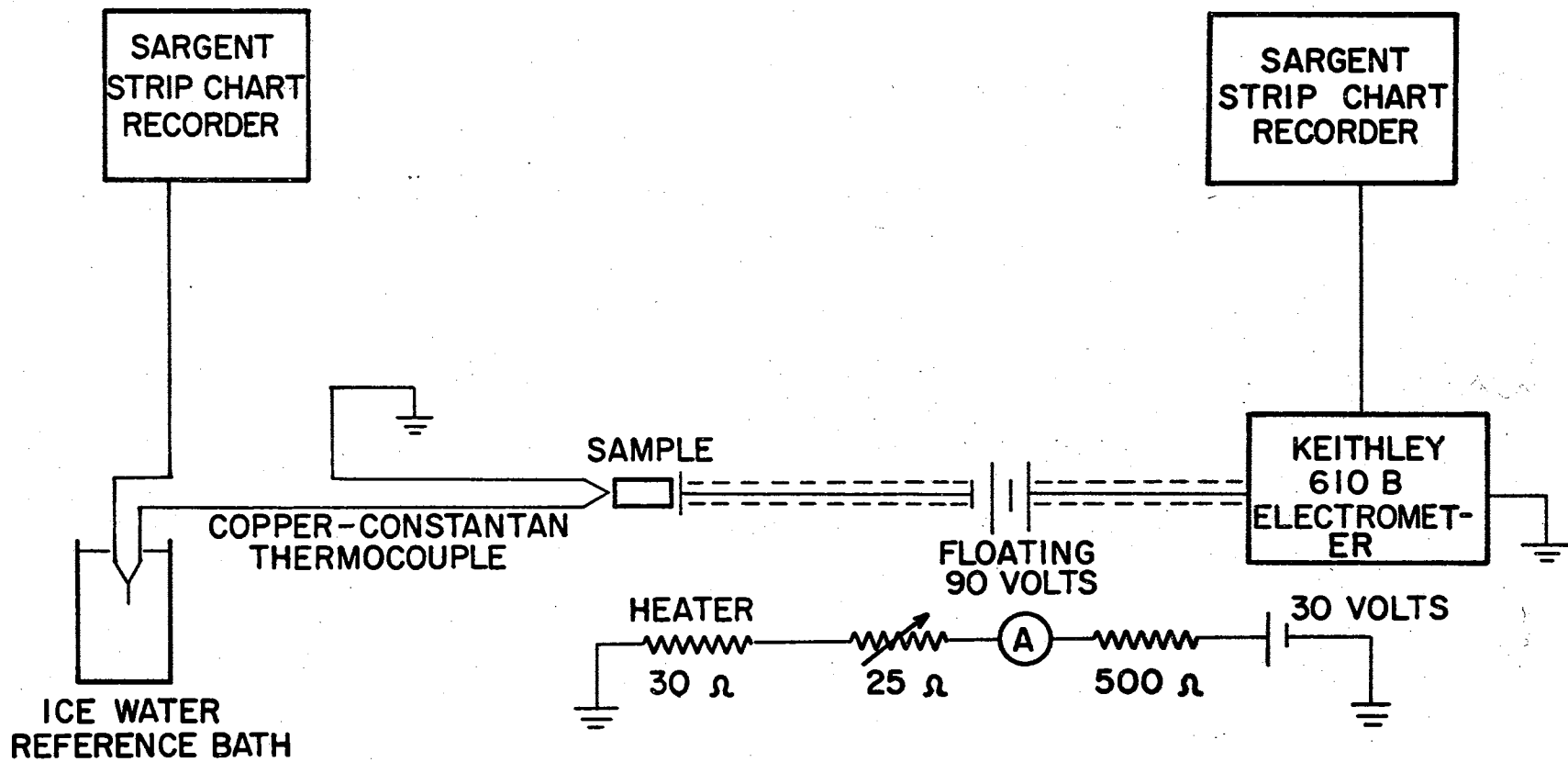


Figure 4. Electrical Measurements-Heater System

Leeds and Northrup and Type #22708(9)-3, made by the Thermo-Electric Co., were provided for convenience in demounting the sample holder. The heater current was monitored with an ammeter placed between the 25 Ω and 500 Ω potentiometers. Using a 30 volt D.C. source, the power dissipated in the heater could be varied from 0-30 watts. A 90 volt floating battery was used to produce a current through the sample using the copper side of the thermocouple as ground. The thermocouple output voltage was monitored on a Sargent Model SR strip chart recorder. The positive side of the floating 90 volt battery was connected to the input of the Keithley 610B electrometer to monitor the sample current. The electrometer output was fed to a second Sargent Model SR strip chart recorder.

The sample holder shown in Figure 5 provided a means of constantly changing the sample temperature and monitoring this temperature change. The sample holder was made of copper tubing which during construction was heated to allow the insertion of the heater wound on a copper spool. The heater wire was asbestos-covered number 28 gage nichrome wire and was grounded to the copper tubing. The "hot" lead to the heater was attached to a vacuum feedthrough to eliminate outgassing effects. The sample was isolated from the copper tubing with a teflon insert and a glass tube was used to support the thermocouple at the lower end of the sample. The copper-constantan thermocouple was run through the glass tubing and a tinned copper cap was soldered to the junction at the base of the sample. A bead of epoxy provided a stop for the spring-loaded glass tubing. Various sizes of samples could thus be accommodated in the sample holder. The upper sample contact was a fixed platinum disc with a fine platinum wire passing through a hole in the teflon insert. The male portion of a miniature connector was attached to this platinum

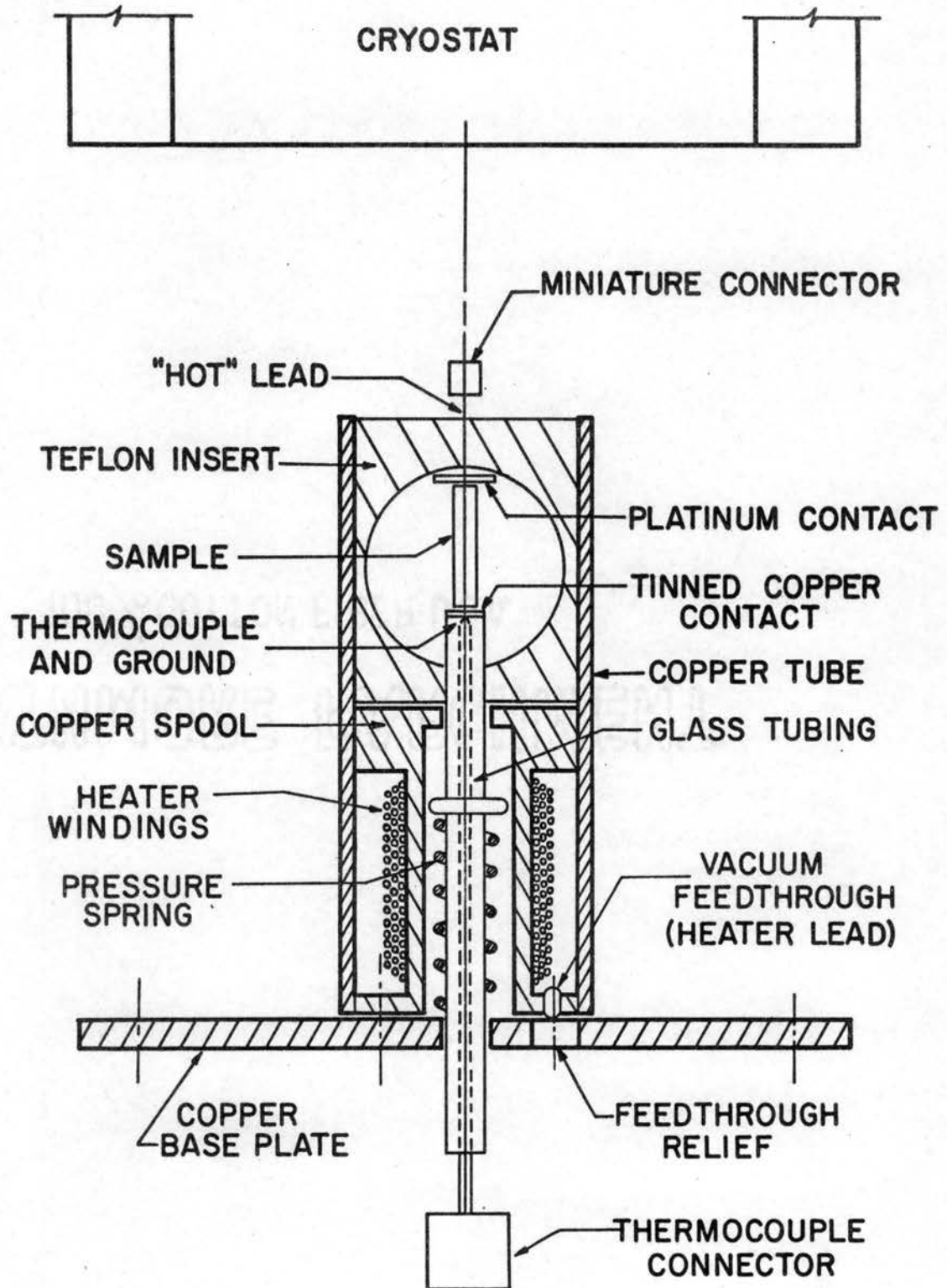


Figure 5. Sample Holder

wire and the female part was attached to the "hot" lead wire emerging from the quartz capillary described earlier. The copper base plate, to which the sample holder was attached with screws, was screwed to the base of the stainless steel dewar to provide a good thermal path to the sample.

The illumination system consisted of a Hg-light source shielded from the eyes by a cylindrical container equipped with an optical port. The optical port could be mounted with screws to the similar port on the outer wall of the cryostat. No lens system was used to concentrate the light since sufficient intensity was obtained by shining the light directly on the sample. Two filters made by Baird-Atomic, Inc., were used to provide the two wavelengths, 3131 \AA and 2536 \AA , used in this investigation.

Samples

The samples studied were rectangular specimens of 0.7% zinc-doped polycrystalline stannic oxide cut from sintered pellets. These pellets were prepared using reagent-grade stannic oxide powder plus 0.7% zinc oxide powder by weight. Specimen pellets were pressed and fired at 1460°C for 4 hours as described by Matthews⁽¹⁴⁾. Samples a few millimeters on a side were cut from the center of these pellets and cleaned using the method described by Rozeboom⁽¹⁵⁾. Silver paint* was applied to the ends of all samples to provide good electrical contacts. These contacts have previously been shown⁽¹⁰⁾ to be ohmic in the range 0 to \pm 100 volts.

* Dupont Silver Preparation, electronic grade #4817.

CHAPTER IV

RESULTS

The discussion of results will be given in two main parts. First the results of the TSC and EWC-TSC will be given and second, the DTSC data will be examined. Prior to each data run, the samples were treated by heating them in a vacuum of 10 microns or in air at one atmosphere pressure for a number of hours at about 100°C. Such treatments are referred to as "fixes". Significant differences were observed in the data from samples fixed for more than 100 hrs when compared with data from samples fixed for less than 100 hrs. For brevity, the former fixing process will be called Fix-A and the latter will be called Fix-B.

A recurring shape was observed in the 0.7% zinc-doped stannic oxide TSC curves for those Fix-B samples heated in a vacuum. When light of $\lambda = 3131\overset{\circ}{\text{A}}$ was used for excitation, two low temperature peaks as shown in Figure 6 were always observed; however, a third peak appeared in some of the data as shown in Figure 7. These three peaks will henceforth be called peak (1), peak (2) and peak (3) respectively, starting with the peak nearest liquid nitrogen temperature. As noted in Figures 6 and 7, peak (1) is greater than peak (2) with peak (2) occurring as a shoulder on the high temperature side of peak (1).

Results similar to those in the last paragraph were observed when the Fix-B samples were heated in air using excitation $\lambda = 3131\overset{\circ}{\text{A}}$ as shown in Figure 8. Here only peak (1) and peak (2) appear, with peak (2)

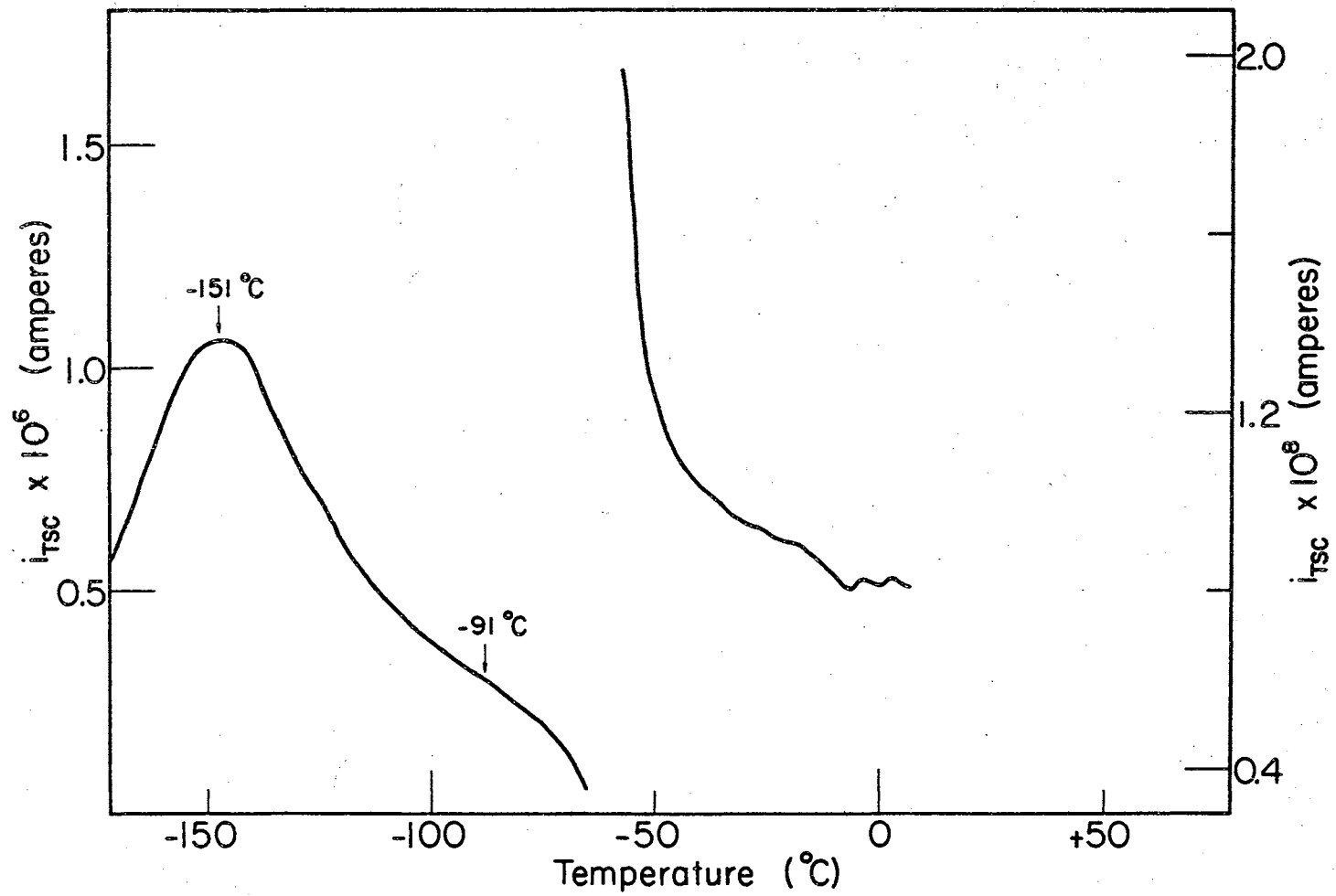


Figure 6. Thermally Stimulated Current of a Fix-B Sample Heated for 47 Hrs at 10 Microns (3131\AA).

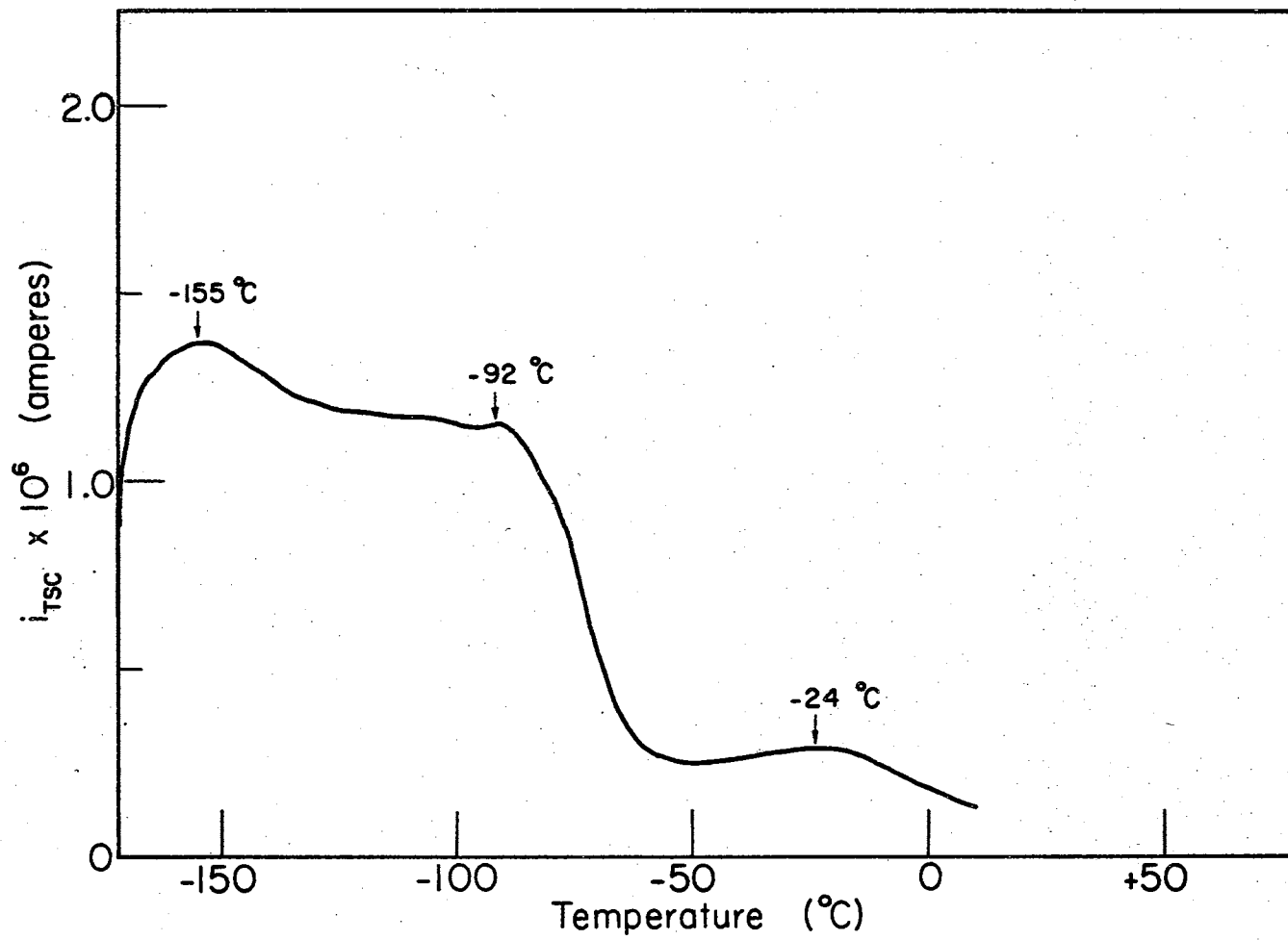


Figure 7. Thermally Stimulated Current of a Fix-B Sample Heated for 46.5 Hrs at 12 Microns (3131\AA).

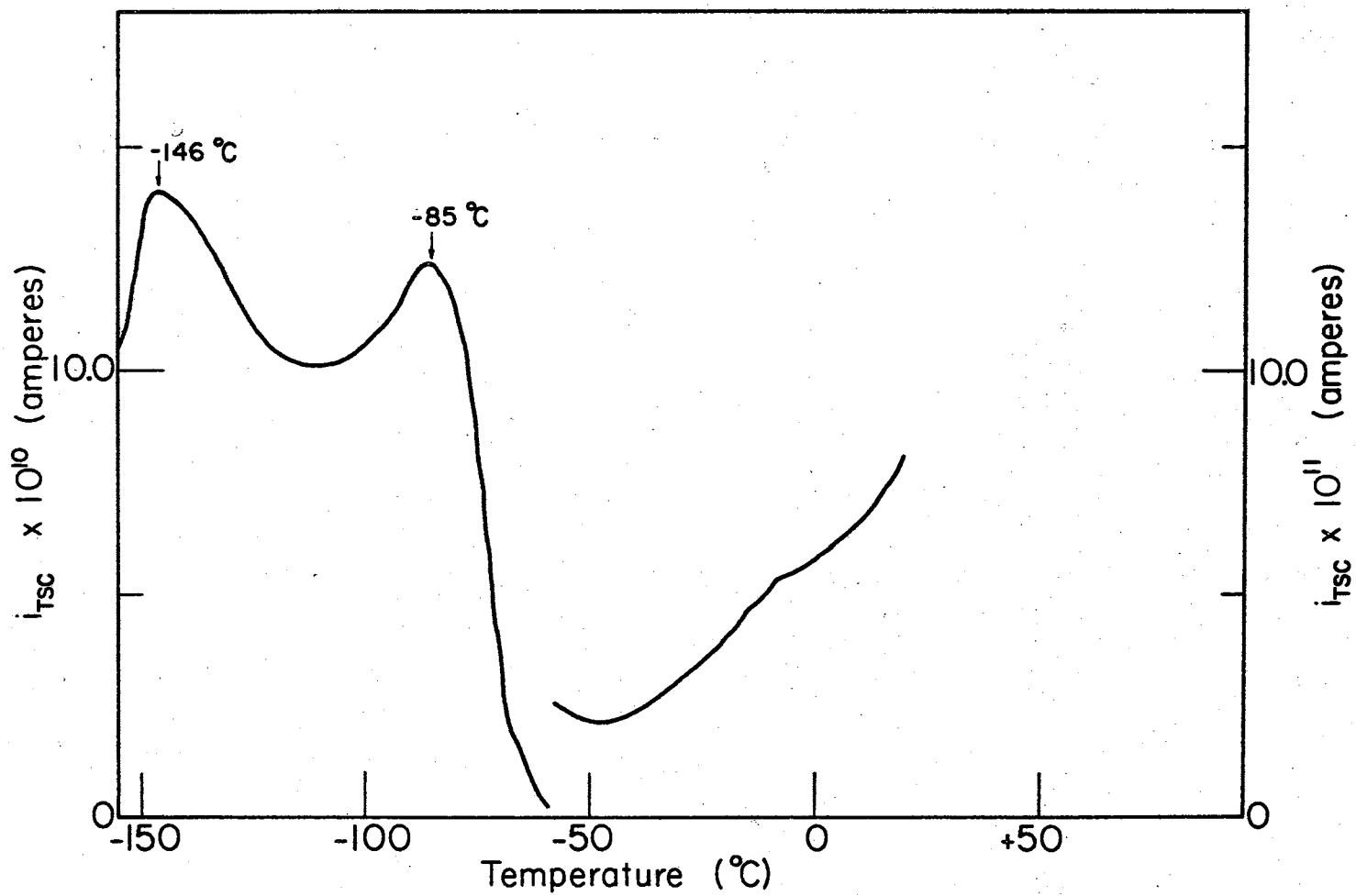


Figure 8. Thermally Stimulated Current of a Fix-B Sample Heated for 10 Hrs in Air (3131A).

being enhanced relative to peak (1) as compared to samples fixed in a vacuum using the same wavelength (Figure 6 and 7). It should be noted that peak (1) is still greater than peak (2) in this case.

The TSC curves of Fix-B samples heated in a vacuum using excitation $\lambda = 2536\overset{\circ}{\text{A}}$ exhibited three peaks as shown in Figure 9. As can be seen, peak (2) is greater than peak (1) with peak (1) appearing as a shoulder on the low temperature side of peak (2). The results of heating in air are shown in Figure 10, where again peak (2) is greater than peak (1). Here it was found that peak (1) was enhanced relative to peak (2) as compared with Fix-B samples heated in a vacuum using the same wavelength (Figure 9).

Fix-A samples, heated in a vacuum, produced TSC curves which differed slightly from those of the Fix-B samples. When $\lambda = 3131\overset{\circ}{\text{A}}$ was used, as noted in Figures 11 and 12, two or three peaks existed but peak (2) was greater than peak (1). Using $\lambda = 2536\overset{\circ}{\text{A}}$, it was noted that peak (1) was enhanced relative to peak (2) when compared with Fix-B samples (Figure 9) although peak (2) still remained greater than peak (1). This is shown in Figure 13. No samples were heated in air for more than 100 hrs, so no data exists for comparison with Fix-A samples heated in a vacuum.

The EWC-TSC curves exhibited the same general shape as the normal TSC curves. The prominent difference was that the sample current was increased above that of the normal TSC run due to the longer excitation time. Fix-B samples heated in a vacuum produced three peaks. After excitation with $\lambda = 3131\overset{\circ}{\text{A}}$, peak (1) was greater than peak (2) with peak (2) appearing as a shoulder on the high temperature side of peak (1) as shown in Figures 14 and 15. Using $\lambda = 2536\overset{\circ}{\text{A}}$, three peaks again appeared

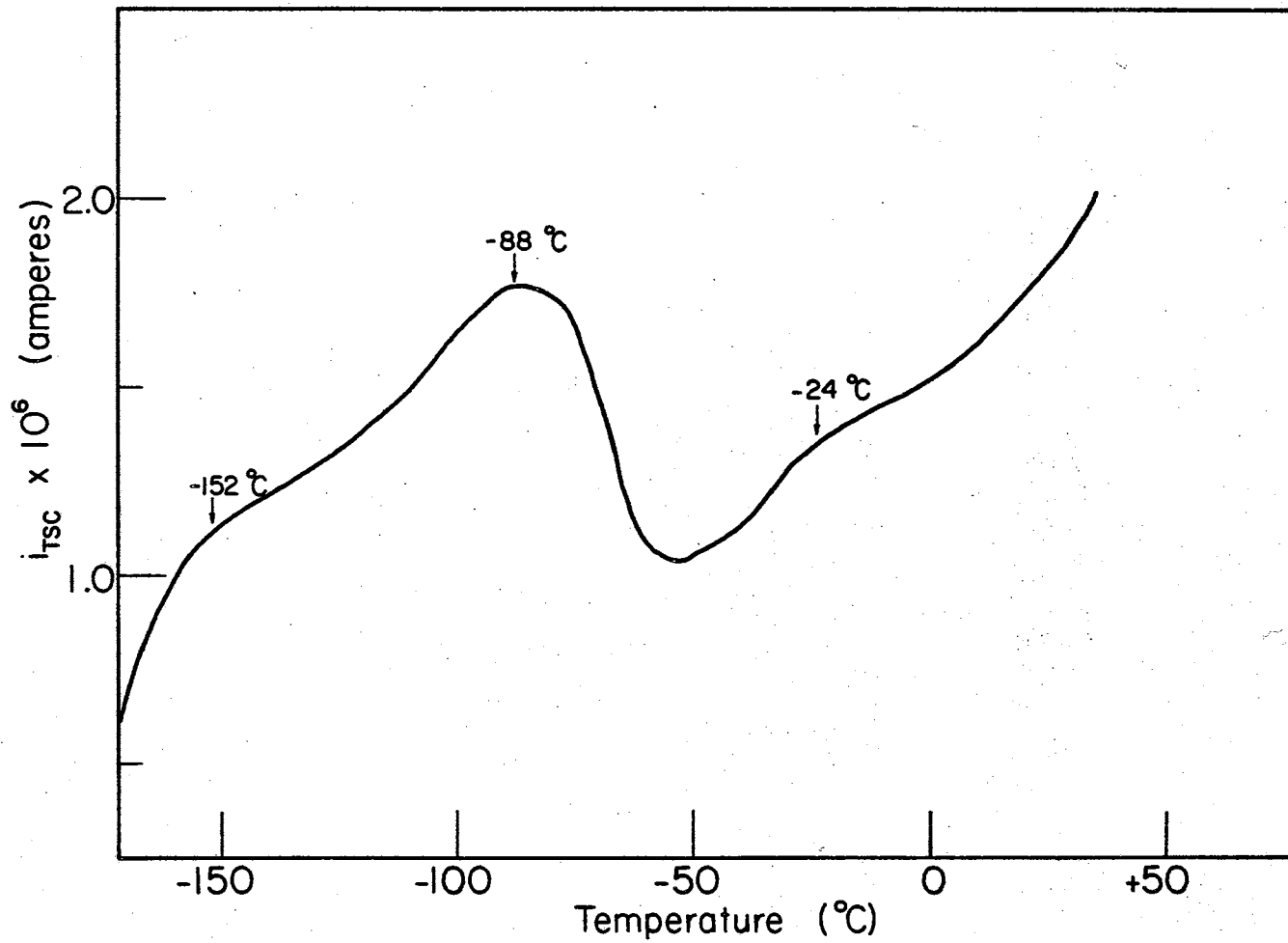


Figure 9. Thermally Stimulated Current of a Fix-B Sample Heated for 46.5 Hrs at 12 Microns (2536Å).

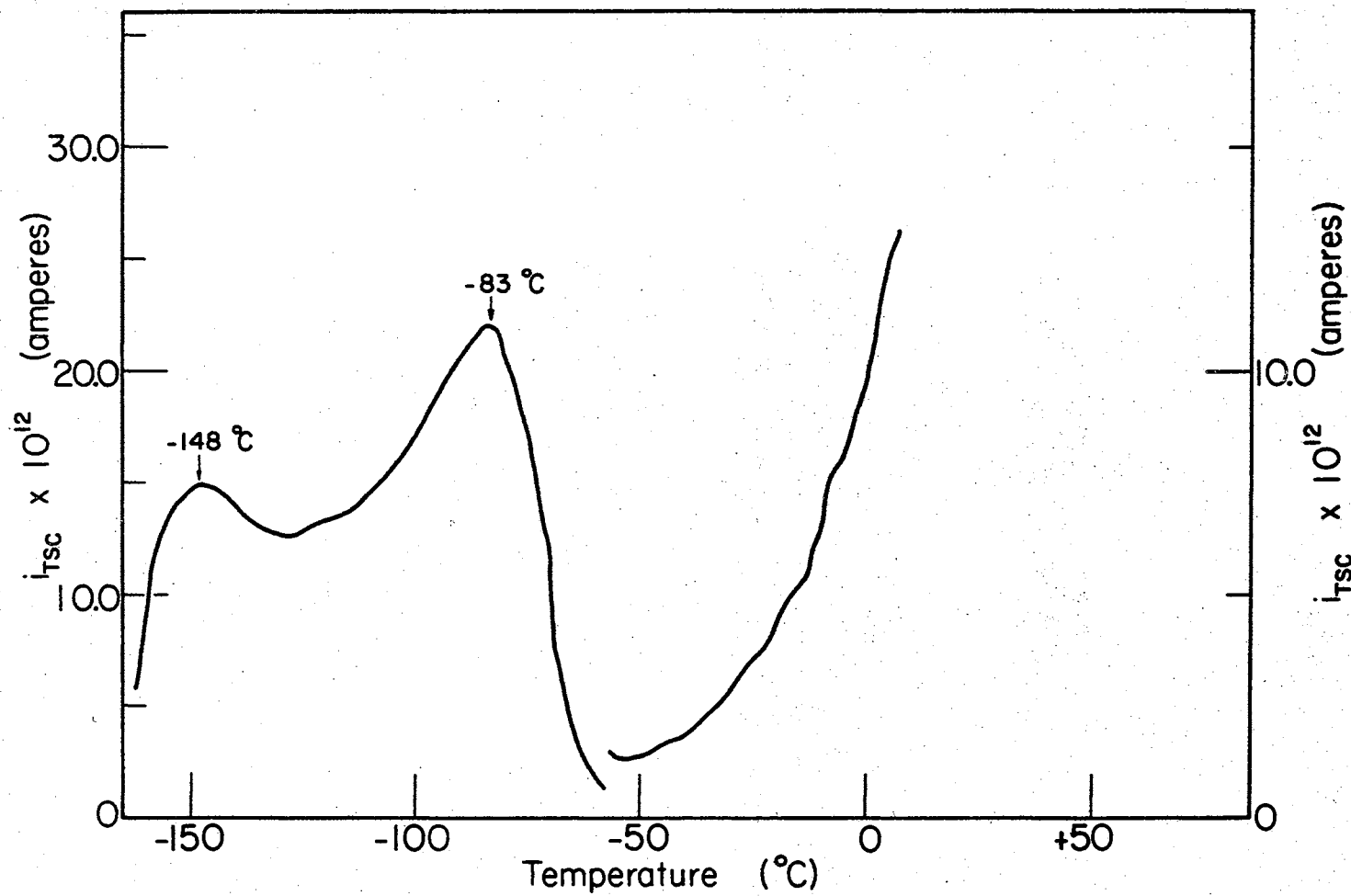


Figure 10. Thermally Stimulated Current of a Fix-B Sample Heated for 10 Hrs in Air (2536A).

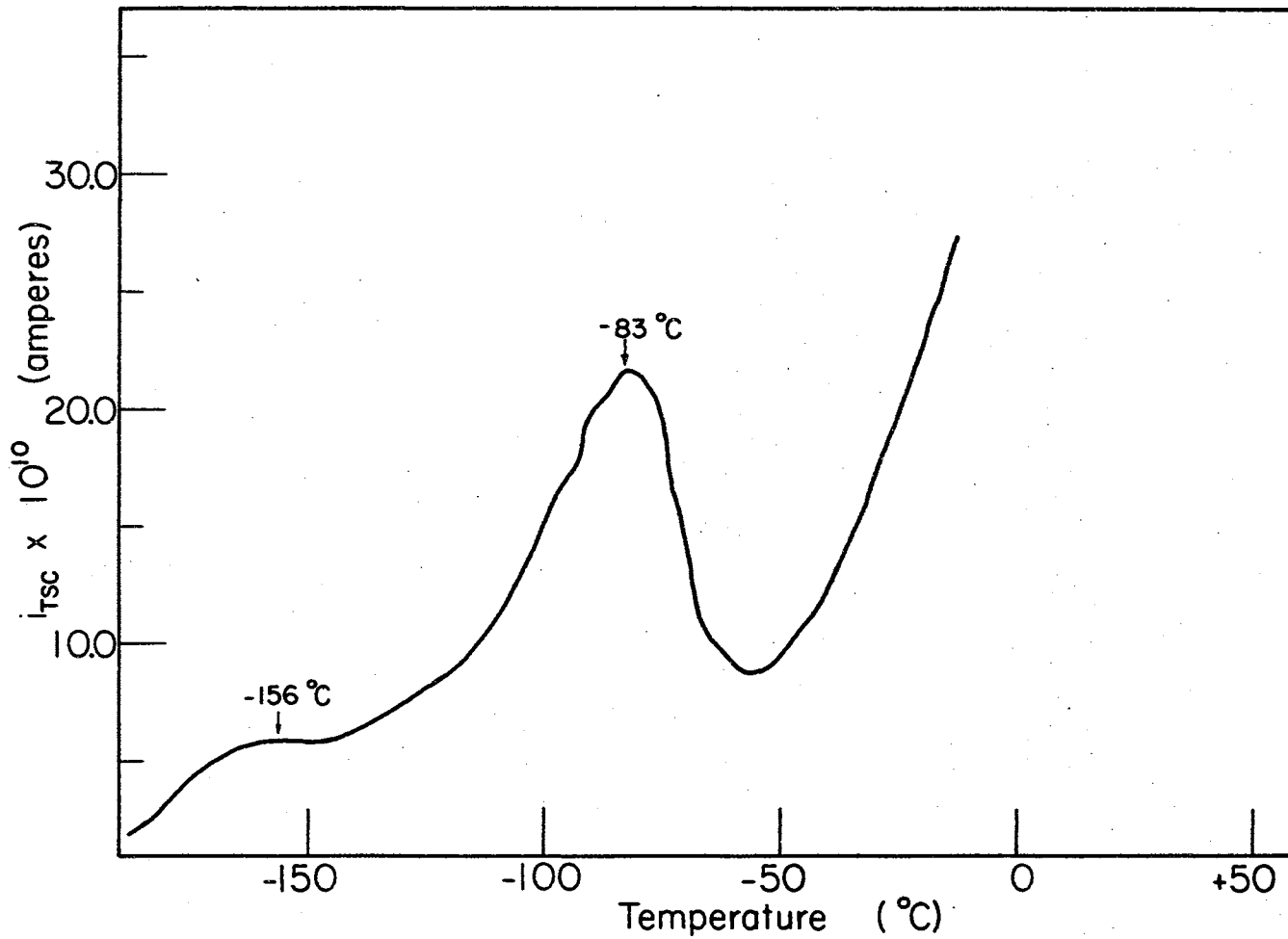


Figure 11. Thermally Stimulated Current of a Fix-A Sample Heated for 120 Hrs at 8 Microns (3131\AA).

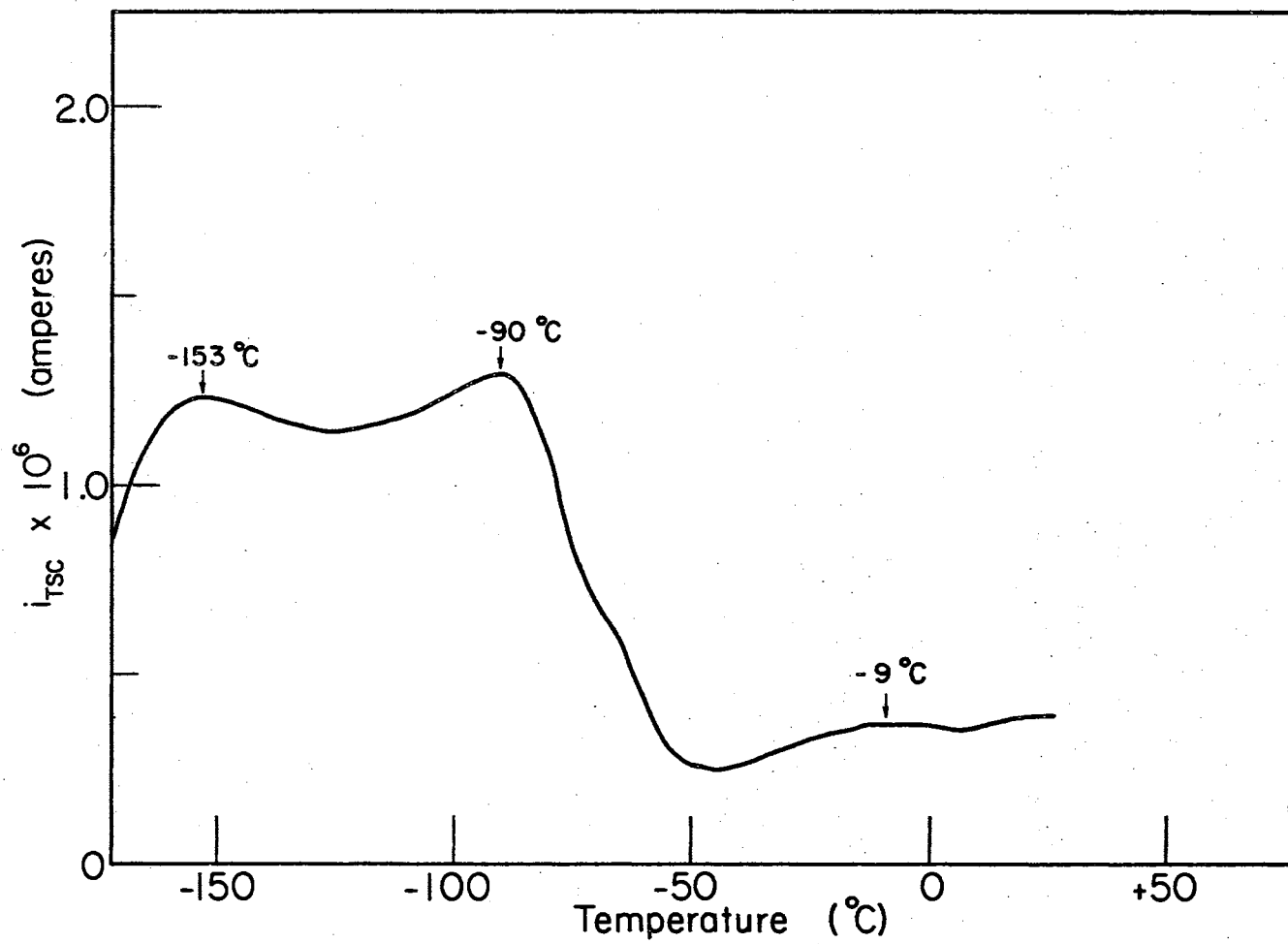


Figure 12. Thermally Stimulated Current of a Fix-A Sample Heated for 114 Hrs at 10 Microns (3131\AA).

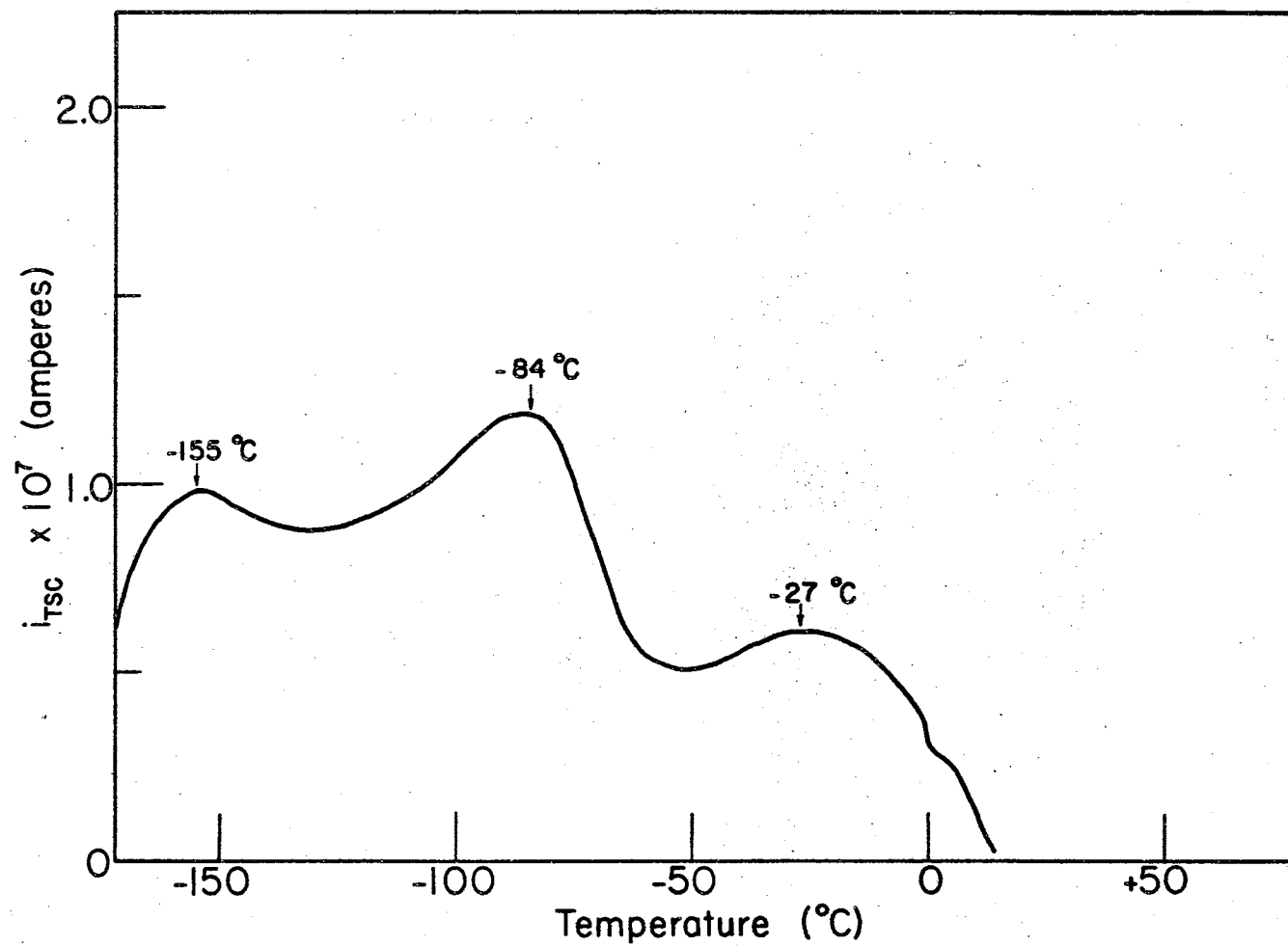


Figure 13. Thermally Stimulated Current of a Fix-A Sample Heated for 114 Hrs at 10 Microns ($2536\overset{\circ}{\text{A}}$).

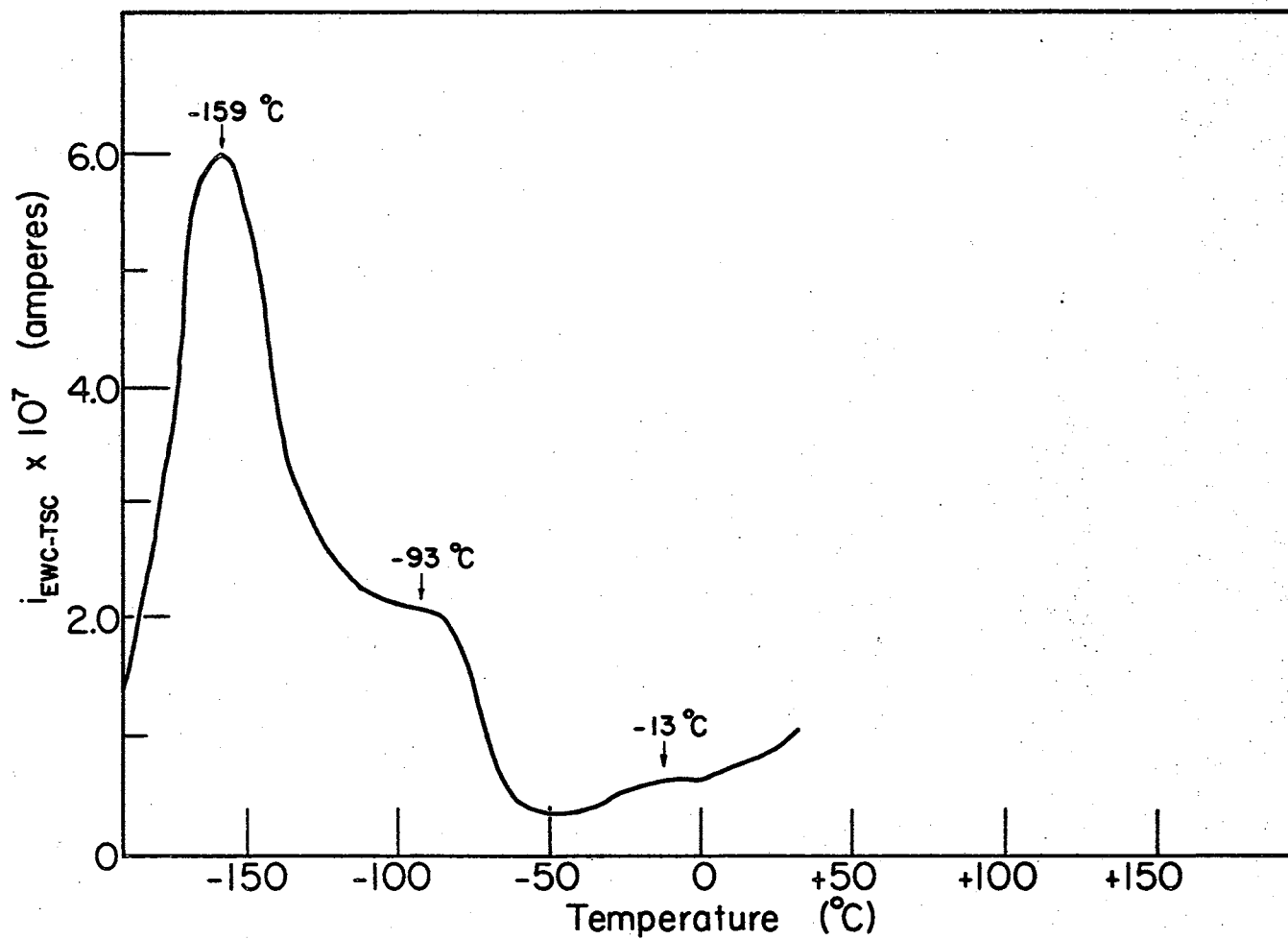


Figure 14. Excitation While Cooling-Thermally Stimulated Current of a Fix-B Sample Heated for 47 Hrs at 10 Microns (3131\AA).

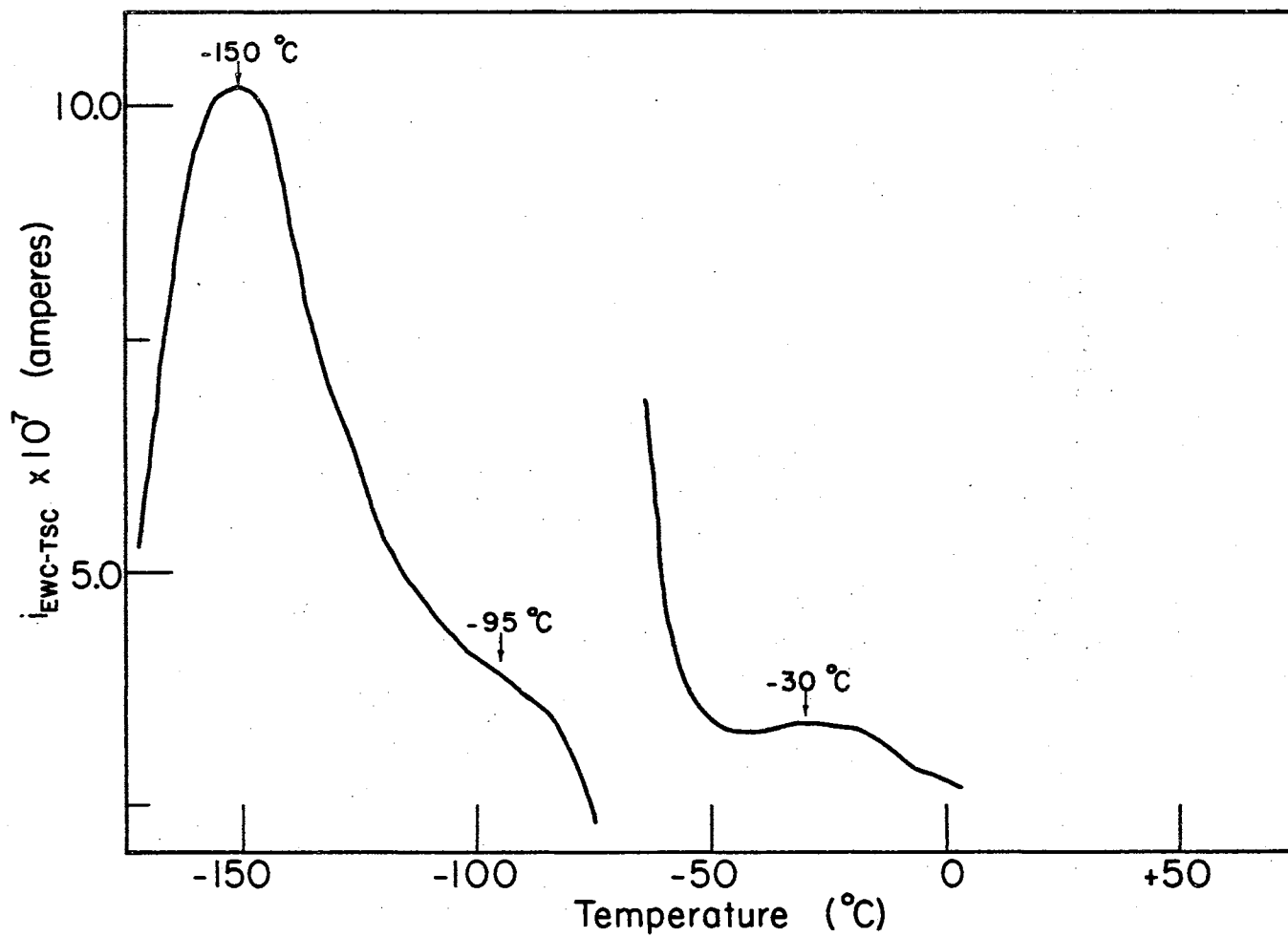


Figure 15. Excitation While Cooling-Thermally Stimulated Current of a Fix-B Sample Heated for 92.5 Hrs at 10 Microns ($3131\overset{\circ}{\text{A}}$).

with peak (2) being greater than peak (1) as shown in Figure 16. These results are therefore in general agreement with those of the corresponding TSC data.

Fix-A samples heated in a vacuum produced three peaks. Figure 17 illustrates that, in comparison with Fix-B samples (Figure 14), a change in the relative height of peak (1) and peak (2) occurred when $\lambda = 3131\text{\AA}$ was used. Here peak (2) was higher than peak (1). Figure 18 shows the results when $\lambda = 2536\text{\AA}$ was used. In this instance, peak (1) was enhanced relative to peak (2) as compared with Fix-B samples (Figure 16), but peak (2) was still greater than peak (1).

Some general observations can be made about all the TSC and EWC-TSC data. The peak temperatures for the salient peaks were variable, but were found to lie within the ranges of -159° to -145°C for peak (1), -96° to -82°C for peak (2) and -27° to -7°C for peak (3). It should be noted that when $\lambda = 2536\text{\AA}$ was used for excitation, peak (2) was always greater than peak (1), whereas when $\lambda = 3131\text{\AA}$ was used, peak (1) was found to be above or below peak (2) depending upon the fixing process.

The DTSC data for peak (1) and peak (2) will now be examined. All determinations of trap activation energies were made using DTSC data. As can be seen from the TSC figures, there was appreciable peak overlap which required thermally decaying away contributions from lower temperature peaks in order to effectively apply the initial rise calculation method. The DTSC method was not applied to peak (3) since preliminary work indicated that a linear plot of $\log i$ versus $1/T$ could not be obtained, presumably because the peak's low current magnitude did not allow sufficient sensitivity for calculation. The data to be discussed first were from Fix-B samples heated either in a vacuum or air.

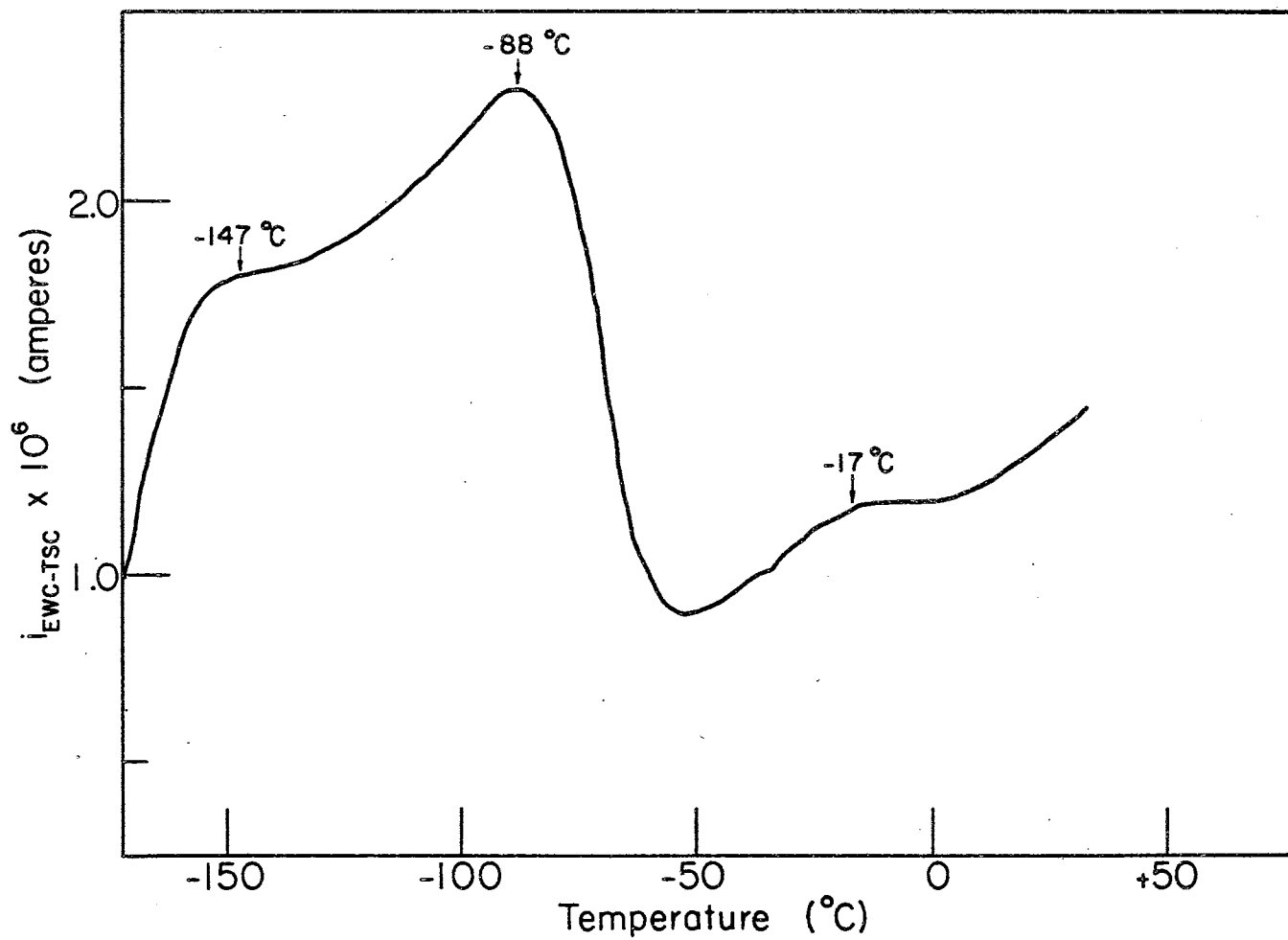


Figure 16. Excitation While Cooling-Thermally Stimulated Current of a Fix-B Sample Heated for 46.5 Hrs at 12 Microns (2536\AA).

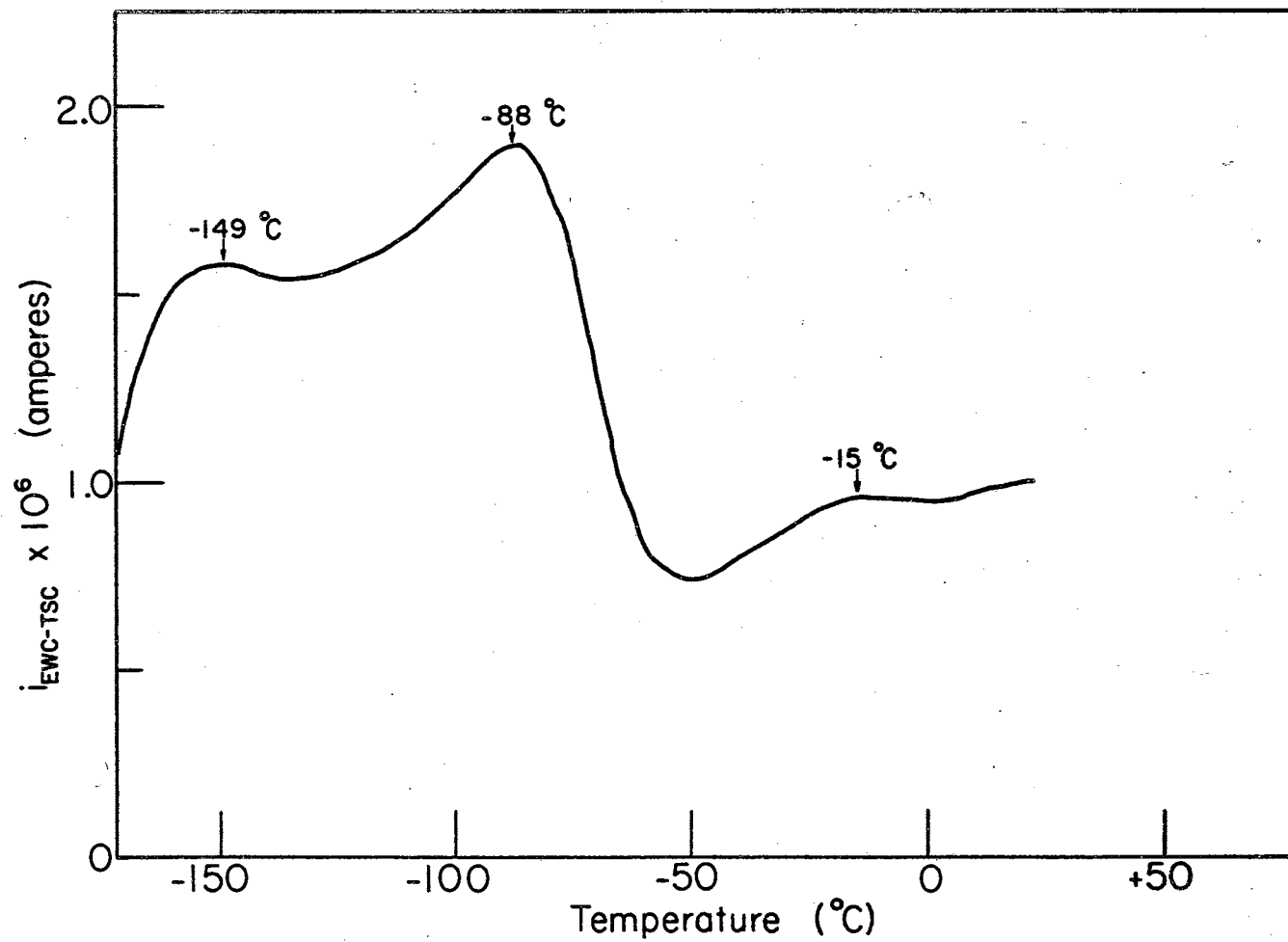


Figure 17. Excitation While Cooling-Thermally Stimulated Current of a Fix-A Sample Heated for 114 Hrs at 10 Microns (3131\AA).

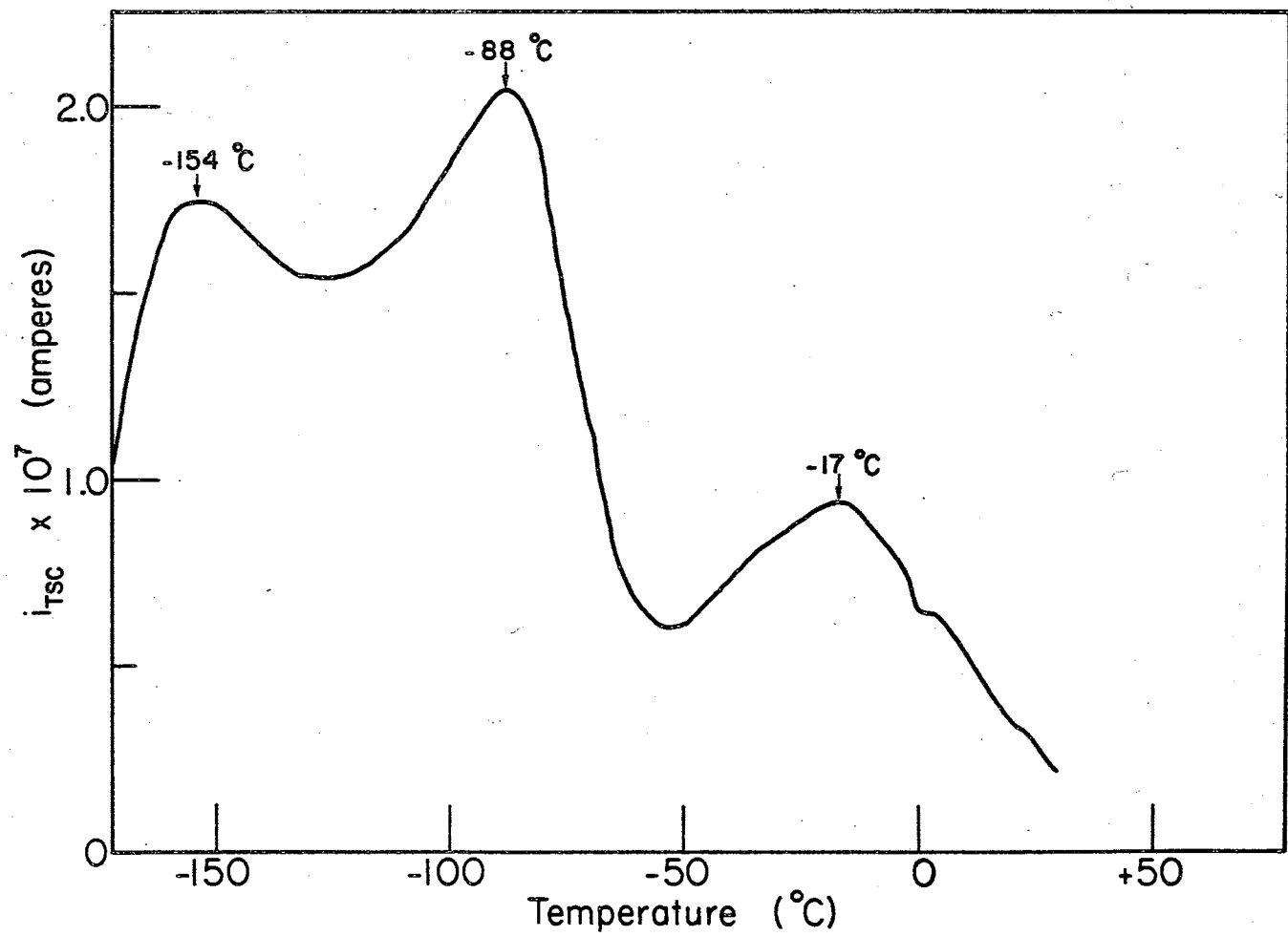


Figure 18. Excitation While Cooling-Thermally Stimulated Current of a Fix-A Sample Heated for 114 Hrs at 10 Microns (2536\AA).

The DTSC data for peak (1) consistently gave a linear plot of $\log i$ versus $1/T$ as shown in Figure 19. The activation energy of peak (1) as found from the slope of such lines ranged from 0.09 ev to 0.12 ev. This spread in the value of the activation energy was primarily a result of decaying to different temperatures prior to the TSC run. A spread in the value of the activation energy was also observed for peak (2) and it was found that for both peaks the activation energies tended to increase as the decay temperature increased. Plots of $\log i$ versus $1/T$ for peak (2) gave an unexpected result. A break in the curve was found in all the data producing two linear portions as shown in Figure 20. Two activation energies were therefore calculated for this peak. A listing of peak temperature, activation energies and decay temperatures for peak (1) and peak (2) is presented in Table I. It should be noted that the

TABLE I

FIX-B ACTIVATION ENERGIES (DTSC) AS A FUNCTION OF DECAY TEMPERATURE

Temperature °C	Energy ev	Decay Temperature °C
Peak (1)		
-144	0.09	-170
-144	0.09	-165
-134	0.09	-163
-133	0.12	-158 (air)
-111	0.12	-141 (air)
Peak (2)		
-93	0.12, 0.09	-117
-89	0.141, 0.105	-108
-87	0.144, 0.107	-102
-86	0.195, 0.134	-105 (air)
-80	0.214, 0.158	- 89 (air)

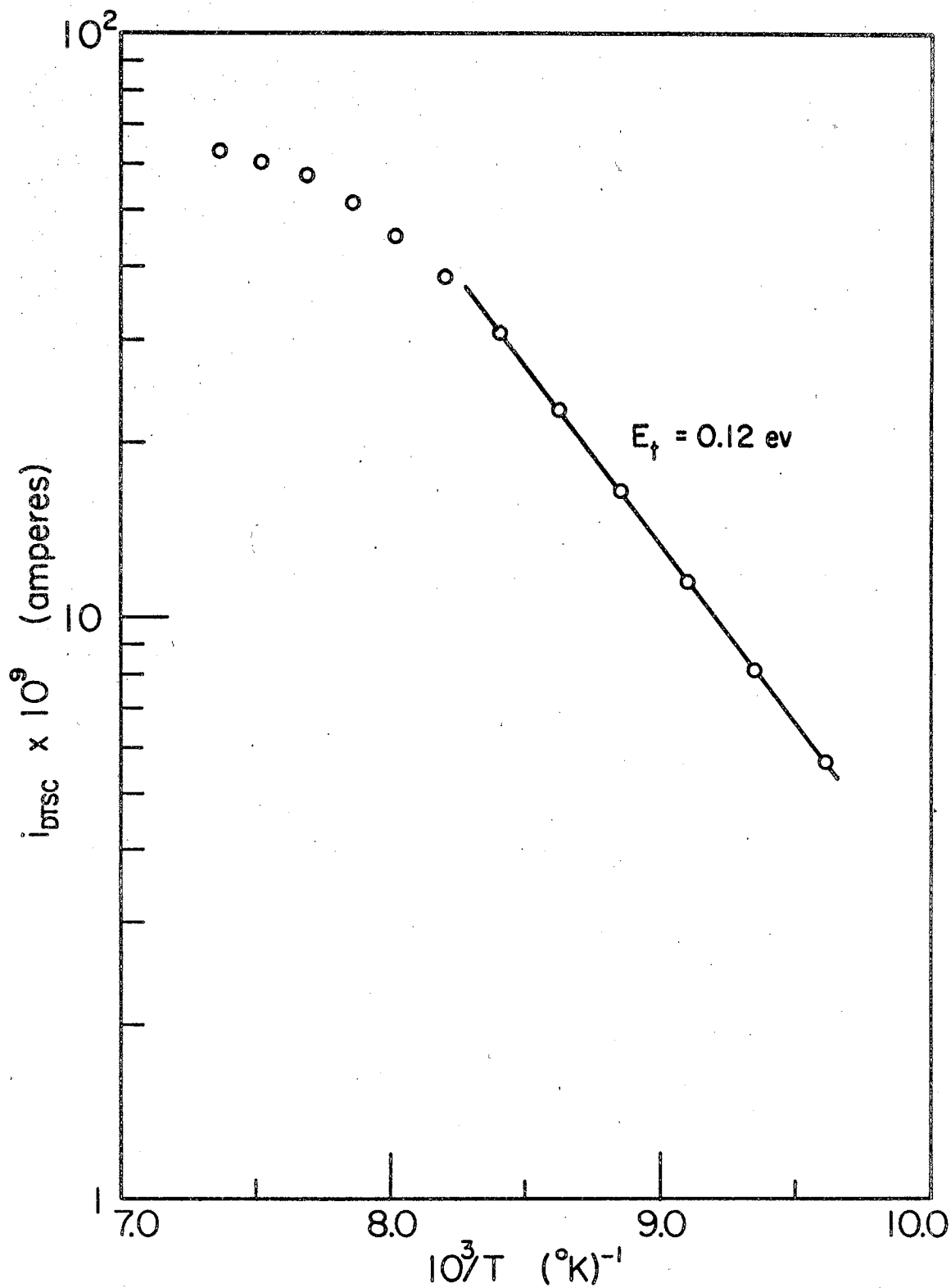


Figure 19. Decayed Thermally Stimulated Current Versus $10^3/T$ for Peak (1) of a Fix-B Sample Heated for 44 Hrs in Air (3131\AA).

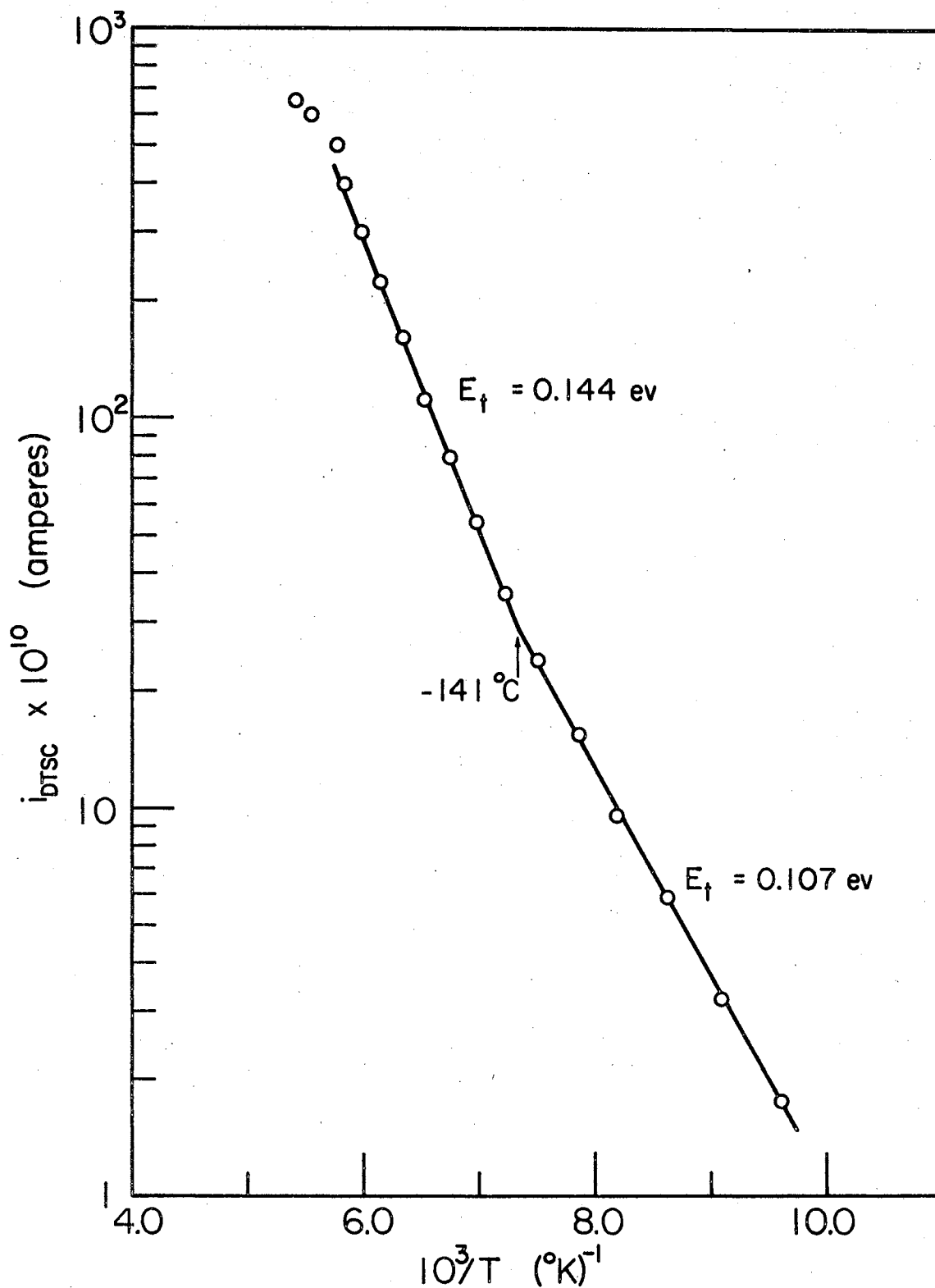


Figure 20. Decayed Thermally Stimulated Current Versus $10^3/T$ for Peak (2) of a Fix-B Sample Heated for 48.5 Hrs at 10 Microns (3131\AA).

apparent peak temperatures listed have been shifted by the decay process to higher values than the ranges set for peak (1) and peak (2) in the discussion of the TSC and EWC-TSC data. This is more noticeable for peak (1) since the placement of peak (2) was less certain due to overlap.

The break temperature between the two linear portions of the $\log i$ versus $1/T$ plot for peak (2) ranged from -150° to -131°C and was observed to increase as the decay temperature increased. This is shown in Table II.

TABLE II
BREAK TEMPERATURES FOR PEAK (2) AS
A FUNCTION OF DECAY TEMPERATURE

Decay Temperature $^{\circ}\text{C}$	Break Temperature $^{\circ}\text{C}$
-117	-150
-106	-143
-105	-143
-102	-141
- 89	-131

Very little DTSC data was taken on Fix-A samples heated in a vacuum, but preliminary runs produced activation energies of 0.104 eV for peak (1) and 0.101 eV and 0.124 eV for peak (2) as shown in Figures 21 and 22 respectively. It should be noted that both these runs were made using $\lambda = 2536\text{\AA}$. It was found that excitation with $\lambda = 3131\text{\AA}$ failed to give data which provided straight lines from which activation energies could be calculated.

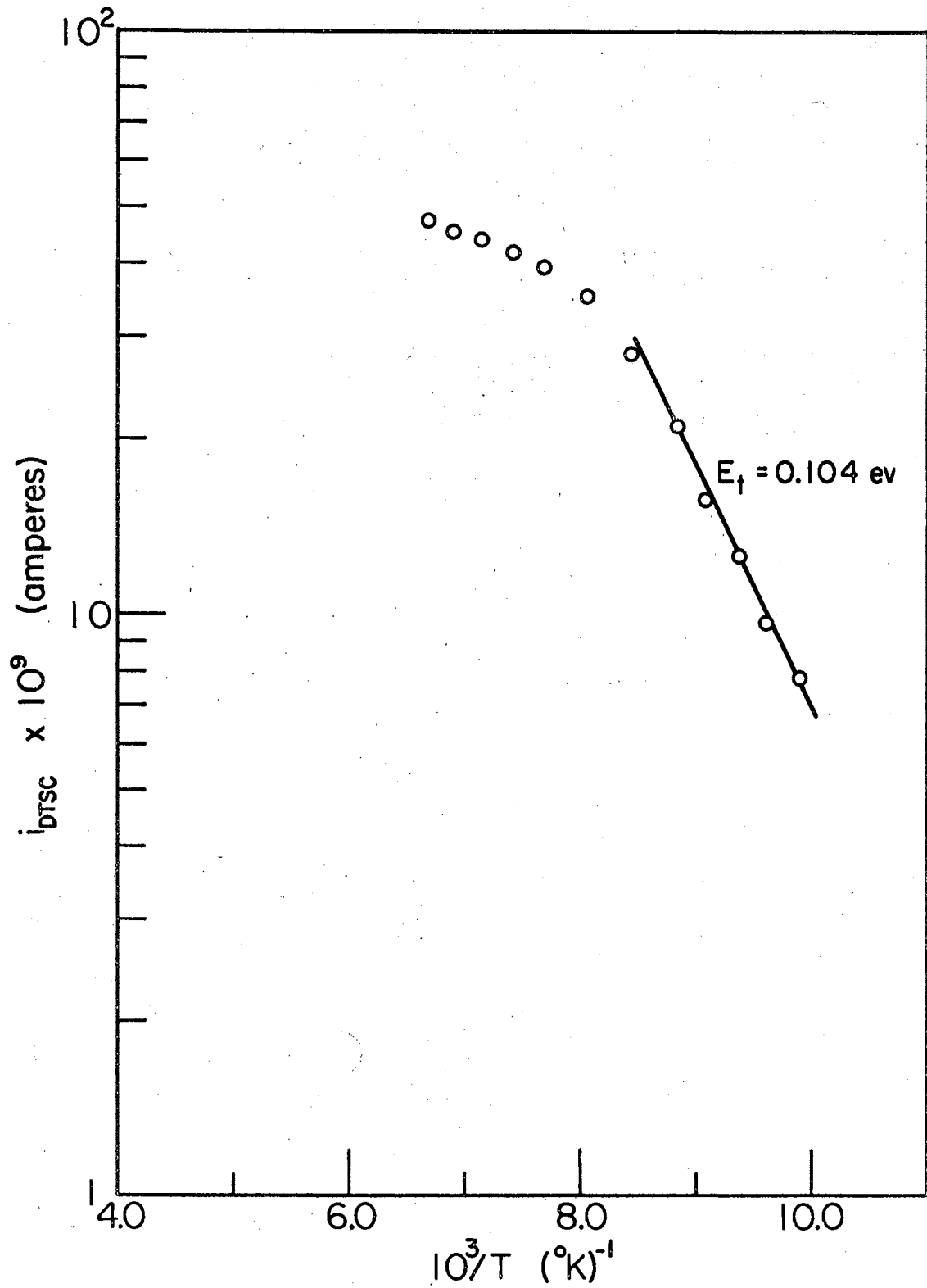


Figure 21. Decayed Thermally Stimulated Current Versus $10^3/T$ for Peak (1) of a Fix-A Sample Heated for 114 Hrs at 10 Microns (2536\AA).

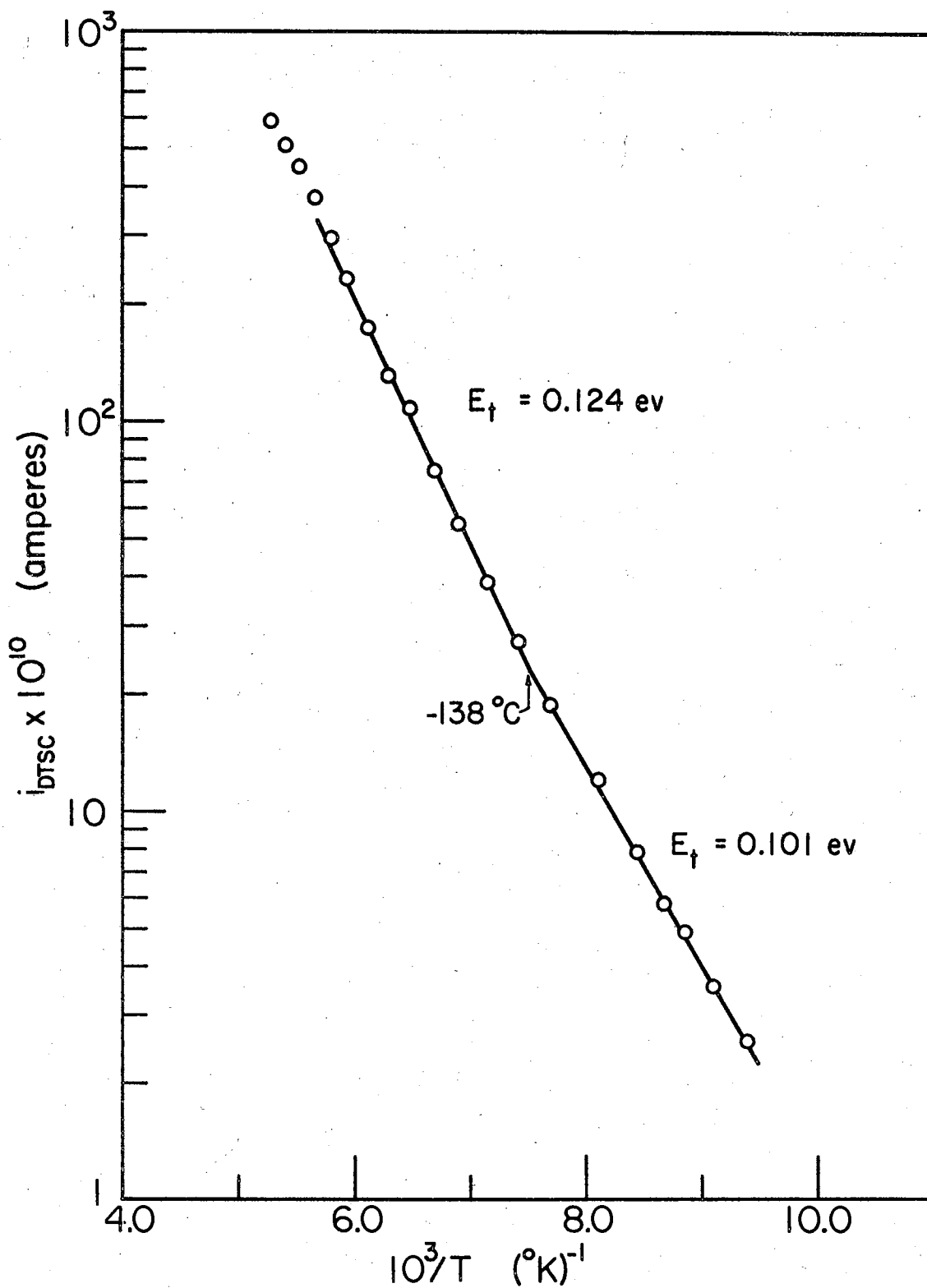


Figure 22. Decayed Thermally Stimulated Current Versus $10^3/T$ for Peak (2) of a Fix-A Sample Heated for 114 Hrs at 10 Microns (2536\AA).

CHAPTER V

DISCUSSION AND CONCLUSIONS

Stannic oxide has been shown to be an n-type semiconductor¹⁶ and the effect of doping it with zinc oxide is to stabilize its properties and increase the sample density. A flat band picture is assumed to apply to this oxide with trapping states whose activation energies lie in the band gap. Such trapping states are assumed to be caused by defects either near the surface or in the bulk of the sample. To investigate these trapping states, two excitation wavelengths ($2536\overset{\circ}{\text{A}}$ and $3131\overset{\circ}{\text{A}}$) have been used. As noted by Matthews¹⁰, radiation of wavelength $\lambda=3131\overset{\circ}{\text{A}}$ penetrates deeper into the sample than the radiation of wavelength $\lambda=2536\overset{\circ}{\text{A}}$. It is therefore assumed that those trapping states near the surface are affected more by $\lambda=2536\overset{\circ}{\text{A}}$ than the trapping states in the bulk whereas all trapping states are affected by $\lambda=3131\overset{\circ}{\text{A}}$.

As noted in the previous chapter, at least three peaks were observed in most of the TSC data. These peaks are assumed to be produced by electrons released from trapping states whose activation energy is below the conduction band edge. The determination of where physically these traps are and what produces them has been the object of the research in this lab and this study is also directed toward that end. An attempt to answer these questions will be based on the results presented in Chapter IV.

Discussion of Results in Fix-B Samples

Certain conclusions can be drawn concerning the relative peak heights in the TSC data. As noted in Figures 6, 7, and 8, peak (1) was greater than peak (2) when wavelength $\lambda=3131\overset{\circ}{\text{A}}$ was used. The most obvious causes of this difference in peak height would be either a greater density of traps associated with peak (1) or a difference in carrier lifetime in the temperature ranges of the two peaks. Work by Matthews¹⁰ and by this investigator using the method of continuous thermal quenching, indicates that the lifetime of the majority carrier does appear to change sharply with temperature in the temperature range of peak (2). Therefore, it will here be assumed that a lifetime change has the dominating effect upon the peak heights but an effect due to a difference in trap density is not completely ruled out.

For future reference, Table III is here presented listing the peak photocurrent attained prior to a TSC run and the ratio of the maximum current for peak (1) to the maximum current for peak (2) for those pertinent figures in Chapter IV.

TABLE III
RELEVANT DATA FOR THE FIGURES IN CHAPTER IV

Figure	Ratio of Height of Peak (1) to Peak (2)	Peak Photocurrent (10^{-6} amperes)
6	3.53	6.20
7	1.24	8.24
8	1.14	0.096
9	0.67	3.16
10	0.74	0.036
11	0.27	0.0009
12	0.82	7.68
13	0.83	0.54
14	2.81	3.20
15	2.61	4.67
16	0.79	4.32
17	0.95	7.20
18	0.86	0.78

Comparing Figure 8 with Figures 6 and 7, one is tempted to relate the slight enhancement of peak (2) mentioned in Chapter IV to the presence of air during the fixing process; but referring to Table III, it is noted that the peak photocurrent for Figure 8 is almost two orders of magnitude less than for Figures 6 and 7. This smaller photocurrent means that fewer electrons have been excited into the conduction band and, therefore, fewer can drop into trapping states. Those dropping into trapping states will preferentially fall to the deepest compensated traps. With more electrons in the trap or traps associated with peak (2), peak (1) will be diminished relative to peak (2) during the TSC run. This effect of low peak photocurrent has been noted by Houston¹⁷. He showed that, using decreasing light intensities to produce different peak photocurrents, a low temperature peak could be depressed relative to higher lying peaks. In the present study shorter excitation times were used to achieve the low peak photocurrents. Also noted in Figure 8, there is better resolution of peak (1) and peak (2) compared with the previous figures. This too agrees with Houston's observation and is tentatively attributed to fewer electrons in total being released from the traps with a consequent reduction of the area under the TSC curve associated with each trap.

The most striking observation when comparing Fix-B samples having been excited with $\lambda=3131\overset{\circ}{\text{A}}$ and $\lambda=2536\overset{\circ}{\text{A}}$ is that there is a reversal in height of peak (1) and peak (2) in going from the longer wavelength to the shorter wavelength as shown in Figures 6 and 9. This might be explained by assuming that peak (2) is associated with a trapping state near the surface which is then more affected by the $\lambda=2536\overset{\circ}{\text{A}}$ radiation. Eagleton¹¹ reached a similar conclusion for two glow peaks occurring at

-140°C and -88°C in his heat treatment studies of thermoluminescence in stannic oxide ceramics. He inferred that higher temperature glow peaks were associated with trapping centers that lay physically closer to the surface because they were more affected by heat treatment procedures.

The enhancement of peak (1) relative to peak (2) noted in Chapter IV for Fix-B samples heated in air using excitation $\lambda=2536\overset{\circ}{\text{A}}$ (compare Figure 10 to Figure 9) again cannot be unambiguously attributed to the ambient air. Referring to Table III it is noted that the enhancement is small (peak height ratio of 0.67 for a fix in vacuum and 0.74 for a fix in air) and that the peak photocurrent is extremely low. Such low currents are comparable with the sample dark current ($\sim 10^{-13}$ amperes). Again the main effect may be that peak (1) and peak (2) are better resolved as a result of the low peak photocurrent.

The EWC-TSC data for Fix-B samples seem to indicate at least three traps as did the normal TSC data. The main significance of using the EWC-TSC method is to investigate the possibility of activated traps which can be filled most easily by shining light on the sample at higher temperatures. Associated with the higher temperatures are phonons which could supply the electrons excited into the conduction band by the incident light with enough energy to overcome the repulsive barrier associated with the activated traps. Since no new peaks appear in the EWC-TSC data it is assumed that such traps are nonexistent in the trap-energy range studied or are unobservable using present methods. Further confirmation of the association of peak (2) with a near-surface trapping state is given by the reversal of peak (1) and peak (2) in going from excitation $\lambda=3131\overset{\circ}{\text{A}}$ to $\lambda=2536\overset{\circ}{\text{A}}$. This can be seen by comparing Figure 16 with Figures 14 and 15.

Discussion of Results in Fix-A Samples

The TSC structure for Fix-A samples confirms the existence of at least three trapping levels but the shape of the curves has been altered. Figure 11 exemplifies the most drastic effect observed when a low peak photocurrent was used. The peak height ratio of 0.27 is the lowest listed in Table III. This effect has been discussed previously.

Figure 12 presents the first case in which peak (1), which for Fix-B samples had been always above peak (2), was below peak (2). The large peak photocurrent for this sample (7.68×10^{-6} amperes) appears to rule out explanations based on low photocurrents given earlier. Comparing Figure 12 with Figure 7, all variables being nearly the same in these two cases, except for fixing time, it is noted that the shift in the peaks is very slight. The use of long fixing times is thought to produce a cleaner sample surface, "cleaner" in the sense that more adsorbed gases are removed. This cleaning effect might have caused the shift in the peak heights but the evidence for such an assumption is insufficient at this time.

The enhancement of peak (1) using excitation $\lambda=2536\overset{\circ}{\text{A}}$ for Fix-A samples (Figure 13) compared to the corresponding Fix-B samples (Figure 9) does not fall into the picture presented thus far. Again this effect is small (peak height ratio of 0.83 for Fix-A sample and 0.67 for Fix-B sample) but the surface cleaning effect of the long fixing times might be related. Further study is needed to clarify this point.

The EWC-TSC data for Fix-A samples also substantiate the existence of at least three trapping levels below 0°C and again do not indicate the existence of activated trapping states. The change of peak height noted when comparing Figure 17 with Figure 14 (Fix-B) is not small but

the comparison can be discounted since the peak photocurrent and the sample current are nearly an order of magnitude greater in Figure 17 than in Figure 14. A reversal of the peak heights, however, has occurred in the same fashion as noted in Figure 12 earlier although the long fixing time again cannot definitely be related to this effect.

The EWC-TSC data shown in Figure 18 indicates enhancement of peak (2) using excitation $\lambda=2536\overset{\circ}{\text{A}}$ when compared with TSC data using excitation $\lambda=3131\overset{\circ}{\text{A}}$. This was noted before and the association of peak (2) with trapping state near the surface was suggested. The previously noted (Chapter IV) enhancement of peak (1) relative to peak (2) as compared to Fix-B samples (Figure 16) could be unfounded since the specification of the peak currents for peaks appearing as shoulders on other higher current peaks is somewhat indefinite. The two peaks are again well resolved as has been observed previously for samples whose TSC currents were below 10^{-6} amperes.

Comparison with TSL Peaks

The range in temperature given for the three peaks in the TSC data is in substantial agreement with Eagleton's work¹¹ on the thermoluminescence of doped and undoped stannic oxide ceramics. He found that 0.7% zinc-doped stannic oxide produced TSL glow peaks at about -155°C , -138°C and -90°C and an undoped sample produced peaks at -160°C , -135°C and -85°C . The highest and lowest values given in his data correspond well to the ranges, -159°C to -145°C and -96°C to -82°C , given previously for peak (1) and peak (2). He was unable to observe peak (3) in these samples possibly because of the low light intensity. A peak lying in the temperature range between peak (1) and peak (2) was observed by Eagleton

as noted above, but the TSC measurements did not reveal such a peak. Possibly, this peak was masked by peak (1) and peak (2) and could not be resolved.

Discussion of DTSC Results

The DTSC data indicates that as the decay temperature increases, the calculated activation energy increases for those peaks in the temperature range from -160°C to -80°C . This is generally true for all three groups of energy values given in Table I. Such increases could be caused by contributions from lower lying peaks that gradually decayed out as the true peak is revealed. It could alternately be inferred that one or more non-discrete bands of trapping states exist below the conduction band edge. By decaying deeper into these bands, higher activation energies would be obtained for the different temperature regions. Such an explanation was proposed by Eagleton¹¹ who found that the activation energies for TSL glow peaks in this temperature range extended from 0.08 eV to 0.10 eV and from 0.18 eV to 0.30 eV.

The break in the DTSC curves for peak (2) suggests that two traps or bands of trapping states exist in this temperature range. This break could be caused by the emptying of the trap or traps associated with the linear portion below the break in the DTSC curve. As the temperature increases beyond the break temperature, the major contribution of electrons to the conduction band would then come from the trap or traps associated with the linear portion of the DTSC curve above the break. Following this picture, the largest activation energies (0.214 eV and 0.158 eV) would correspond to the deepest trapping states in the two bands associated with the two groups of activation energies for peak (2).

The small amount of DTSC data taken on Fix-A samples indicated no deviations from the results on the Fix-B samples. The activation energies fell with the three groups of values given in Table I.

Additional Comments and Suggestions for Further Study

As in any study of this nature, many variables are involved which have a bearing on the results. An attempt was made to restrict the number of variables so that conclusions could be drawn about the parameters related to the conductivity properties of stannic oxide, but a more limited study seems to be indicated.

The major problem encountered in this investigation was resolving overlapping peaks so that the initial rise method could be used to calculate activation energies. An extension of this work could involve using lower peak photocurrents which might cause the TSC peaks to be better resolved and might disclose peaks unseen before. Of prime importance in the study of stannic oxide is the effect of gases adsorbed on the surface. More work needs to be done to specify the nature of the adsorbed gases. By adding different dopants and using various heat treatments, knowledge of the physical location of the trapping states and their chemical origin might be gained. The heating rate used in this study (~ 0.05 °C/sec) could have affected the structure and the temperature of the TSC peaks. Studies using different heating rates might indicate the nature of these effects.

BIBLIOGRAPHY

1. Peterson, A. F., Ph.D. dissertation, Rutgers University (1968).
2. Bube, R. H., J. Appl. Phys., 35, 586 (1964).
3. Kulp, B. A., J. Appl. Phys., 36, 553 (1965).
4. Haering, R. R. and Adams, E. N., Phys. Rev., 117, 451 (1960).
5. Dittfield, H. J. and Voigt, J., Phys. Status Solidi, 3, 1941 (1963).
6. Nicholas, K. H. and Woods, J., Brit. J. Appl. Phys., 15, 783 (1964).
7. Bube, R. H., J. Appl. Phys., 35, 3067 (1964).
8. Houston, J. E. and Kohnke, E. E., J. Appl. Phys., 37, 3083 (1966).
9. Houston, J. E. and Kohnke, E. E., J. Appl. Phys., 36, 3931 (1965).
10. Matthews, H. E., Ph.D. dissertation, Oklahoma State University (1967).
11. Eagleton, R. D., Ph.D. dissertation, Oklahoma State University (1968).
12. Bube, R. H., Photoconductivity of Solids, John Wiley and Sons, New York (1960).
13. Garlick, G. F. J. and Gibson, A. F., Proc. Roy. Soc. (London), A60, 574 (1948).
14. Matthews, H. E., Unpublished Master's Thesis, Oklahoma State University (1965).
15. Rozeboom, V. E., Unpublished Master's Thesis, Oklahoma State University (1968).
16. Marley, J. A. and Dockerty, R. C., Phys. Rev., 140, A304 (1965).
17. Houston, J. E., Photoelectronic Analysis of Imperfections in Grown Stannic Oxide Crystals, Tech. Rept. #4, Feb. 1965, Contract #Nor-2595 (01).

VITA

John Allen Freeman

Candidate for the Degree of

Master of Science

Thesis: THERMALLY STIMULATED CONDUCTIVITY OF ZINC-DOPED POLYCRYSTALLINE
STANNIC OXIDE

Major Field: Physics

Biographical:

Personal Data: Born in El Reno, Oklahoma, March 23, 1944, the son
of John and Wilma Freeman.

Education: Graduated from Putnam City High School in Oklahoma
City, Oklahoma, in 1962; received a Bachelor of Science degree
from Oklahoma State University, Stillwater, Oklahoma, with a
major in Physics in June, 1966.